'Omics Prospects in Ecological Risk Assessment (OPERA)

Christer Hogstrand
King's College London

Peter Kille
Cardiff University

Technology Solutions and Challenges

GA 2000/2500

2010-2016

MiSeq

Nanopore

PacBio RS II

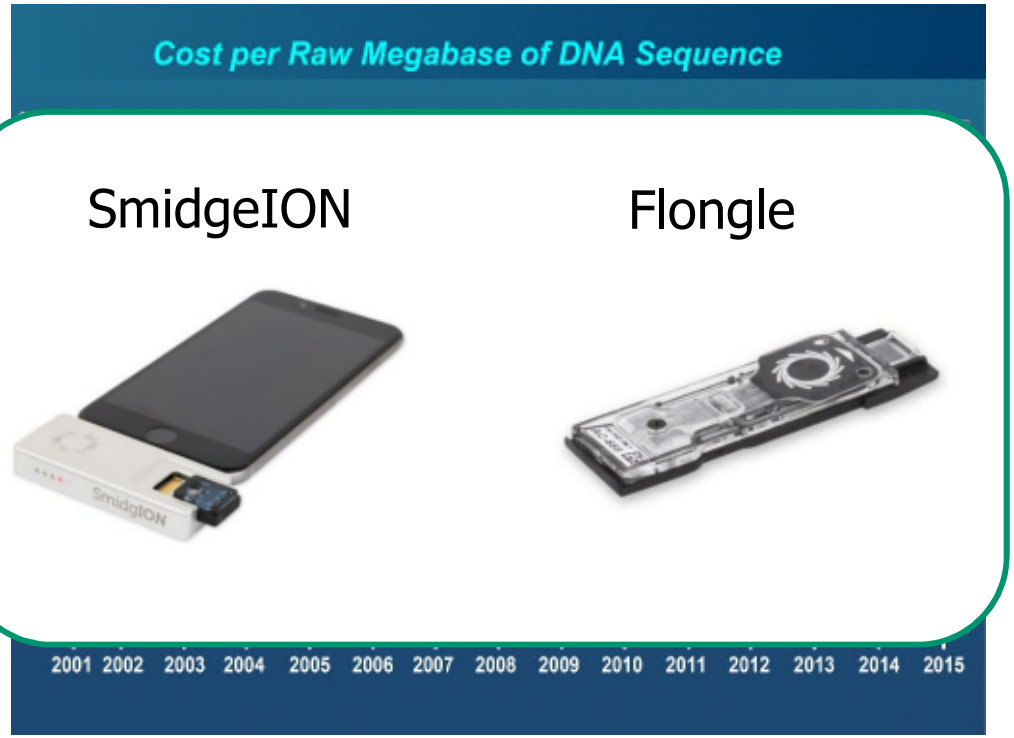

Illumina 4000

Proton

Genome resources are increasing very rapidly beyond classic model organisms to "non-model" species

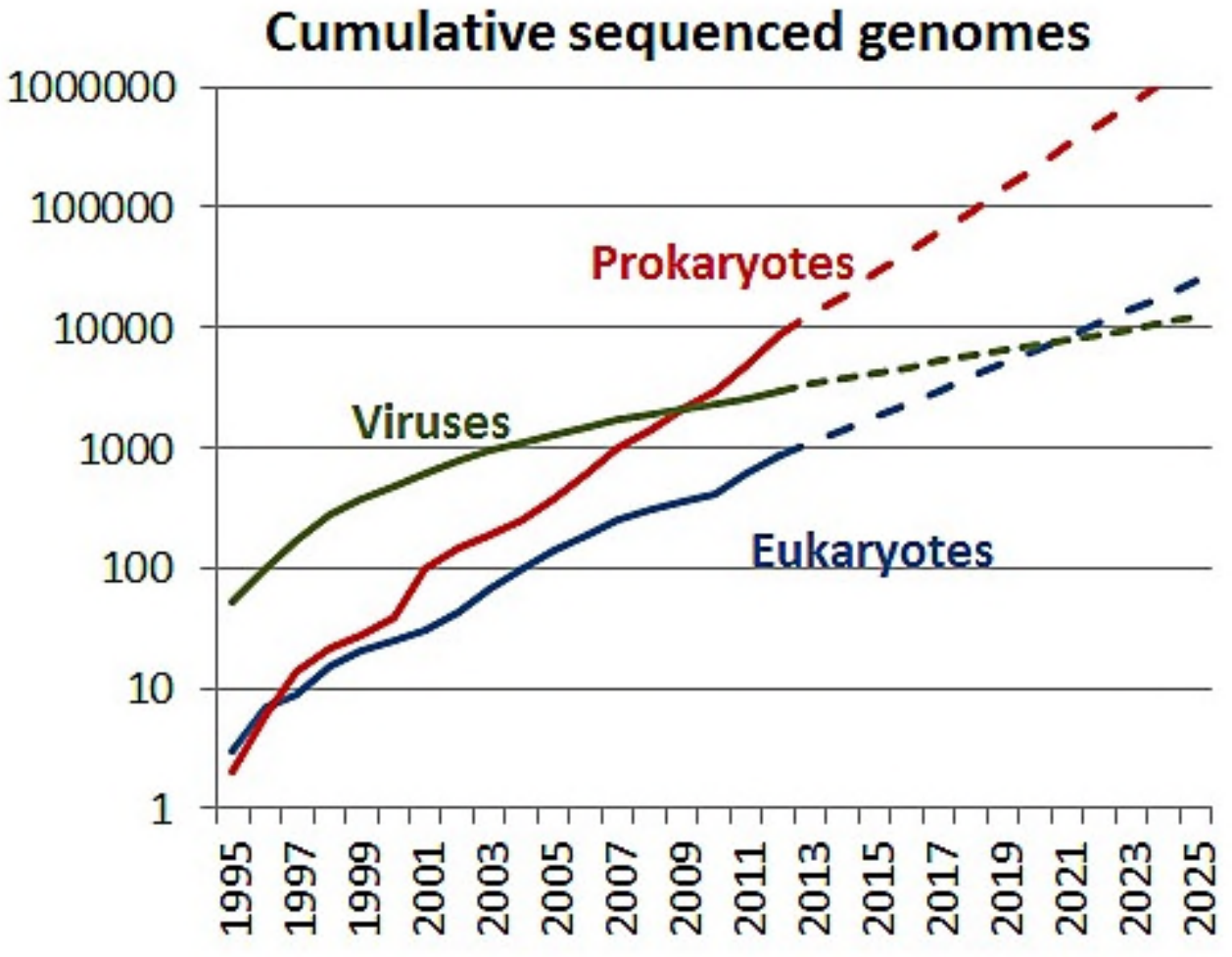

Areas of 'Omics Delivery

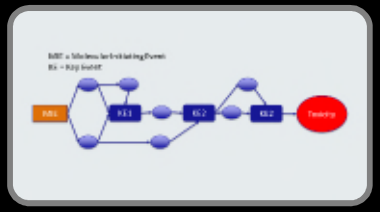

Sub-lethal 'effect pathways' informing MoA and AOP

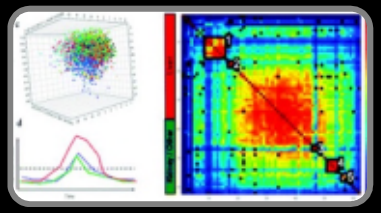

Chemical classification and grouping

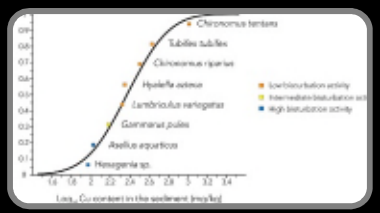

Read-across to estimate different species sensitivities

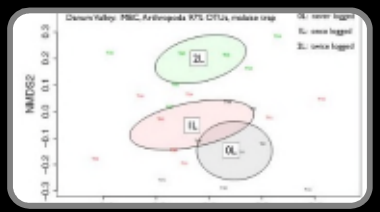

Community and ecosystem impact

(Retrospective monitoring)

Sub-lethal ‘effect pathways’: MoA and AOP

Toxic responses are not static

Transcriptome responses are very dynamic

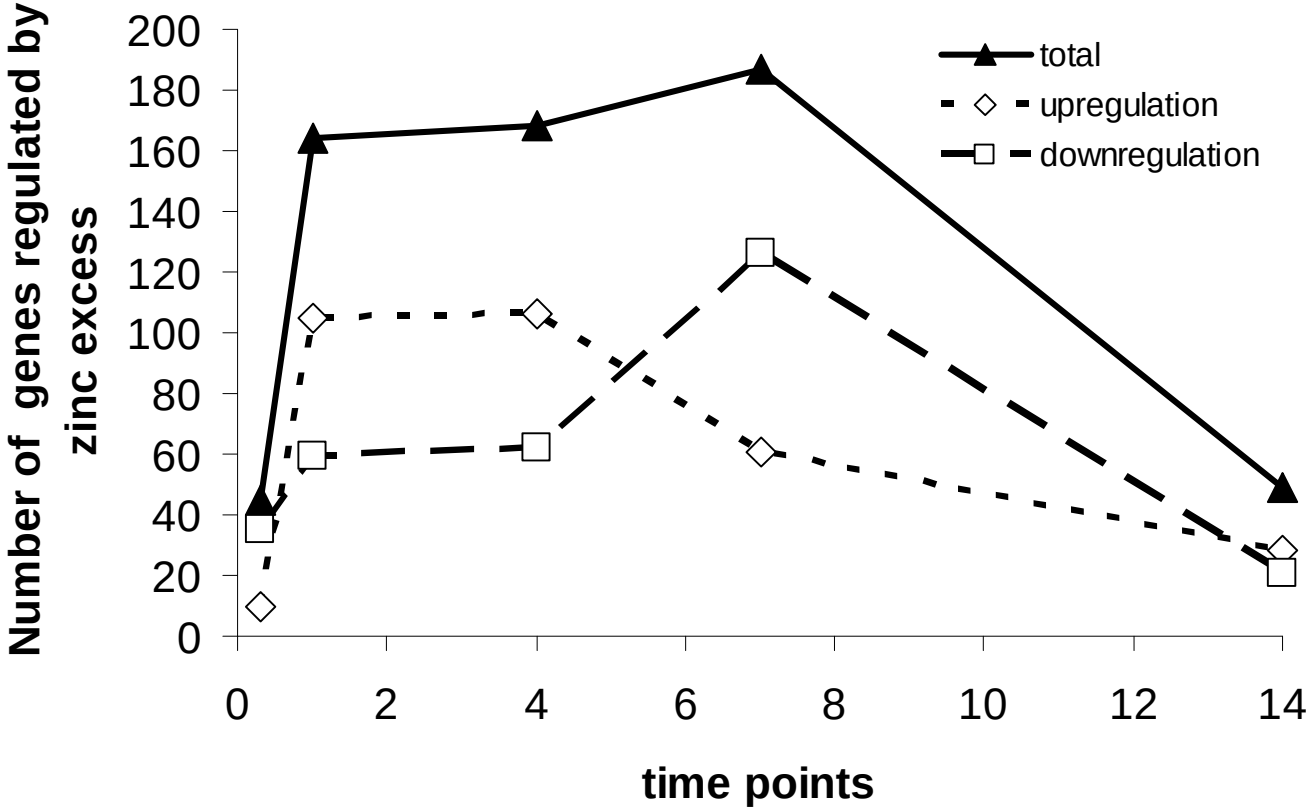

mRNA expression responses ripple through the genome over time

Zheng et al. (2010) BMC Genomics 11:553

Annotation Clusters	Category Name	Genes	Enrichment on day 0.3	1	4	7	14	P-value
Development								
BP	developmental process	96						7.4E-06
BP	anatomical structure development	68						3.6E-05
BP	system development	54						6.2E-04
BP	multicellular organismal process	97						1.1E-03
BP	nervous system development	29						1.2E-03
BP	cellular developmental process	53						2.7E-03
BP	cell differentiation	53						2.7E-03
BP	cell development	39						3.1E-03
BP	multicellular organismal development	64						3.4E-03
BP	brain development	10						3.9E-03
BP	central nervous system development	13						4.7E-03
BP	organ development	39						5.0E-03
BP	cell fate commitment	7						7.4E-03
Metabolism								
BP	primary metabolic process	197						1.1E-05
BP	metabolic process	213						1.2E-05
BP	cellular metabolic process	196						1.5E-05
BP	lipid biosynthetic process	14						3.0E-03
BP	biopolymer metabolic process	126						4.9E-03
BP	macromolecule metabolic process	161						8.2E-03
BP	multicellular organismal catabolic process	4						8.3E-03
Gene expression								
MF	sequence-specific DNA binding	28						7.6E-06
BP	transcription from RNA polymerase II promoter	28						2.4E-04
BP	positive regulation of nucleobase, nucleoside, nucleotide and nucleic acid metabolic process	16						2.3E-03
MF	transcription factor activity	33						3.0E-03
BP	positive regulation of transcription	15						4.4E-03
BP	positive regulation of transcription, DNA-dependent	13						5.1E-03
MF	transcription factor binding	17						5.3E-03
Nuclear receptors								
BP	response to steroid hormone stimulus	6						6.8E-04
MF	steroid hormone receptor activity	6						5.0E-03
MF	retinol binding	3						8.9E-03
MF	ligand-dependent nuclear receptor activity	6						9.0E-03
Regulation								
BP	positive regulation of biological process	38						7.2E-04
BP	positive regulation of cellular process	33						3.2E-03
BP	regulation of multicellular organismal process	14						4.5E-03
BP	regulation of biological process	114						4.7E-03
BP	biological regulation	122						8.3E-03
Others								
MF	oxidoreductase activity, acting on paired donors, with incorporation or reduction of molecular oxygen	9						3.0E-03
BP	microtubule cytoskeleton organization and biogenesis	7						5.3E-03
BP	cell cycle process	26						5.5E-03
MF	5'-nucleotidase activity	3						6.7E-03
MF	oxygen binding	5						6.8E-03
MF	iron ion binding	14						7.3E-03
MF	nucleotidase activity	3						8.9E-03
BP	detection of abiotic stimulus	5						9.2E-03

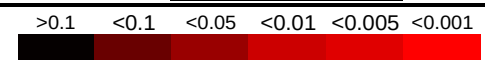

Development

Metabolism

Gene expression

Nuclear receptors

Regulation

Others
(e.g. Cell cycle process, iron binding, microtuble cytoskeleton organisation)

Zheng et al. (2010) BMC Genomics 11:553

Time-dependent expression of genes in main enriched categories

Sequence-specific DNA binding

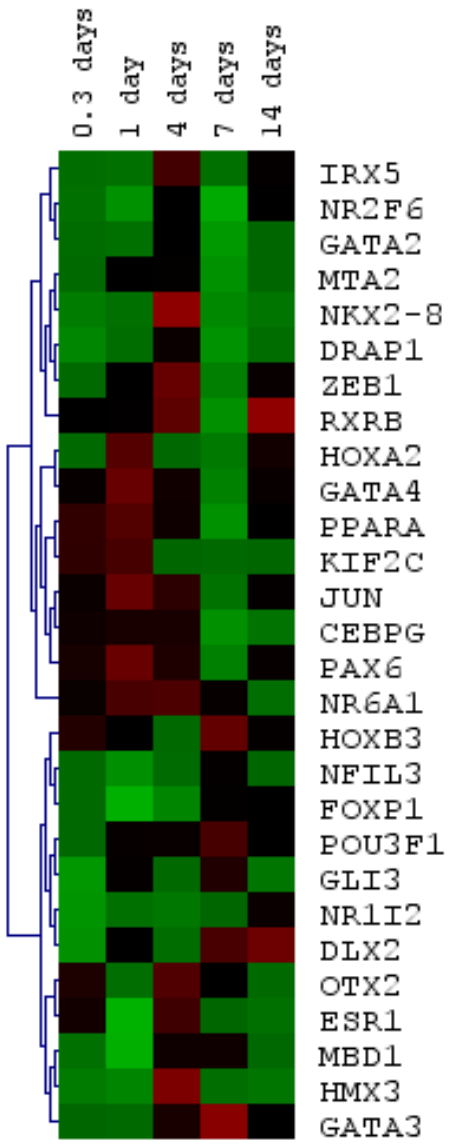

Nervous system development

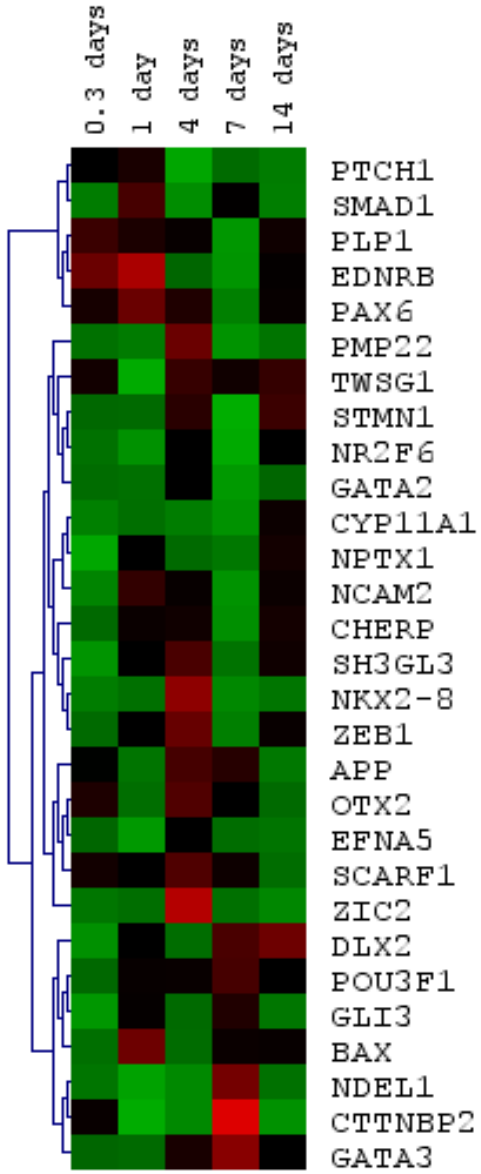

Lipid biosynthetic process

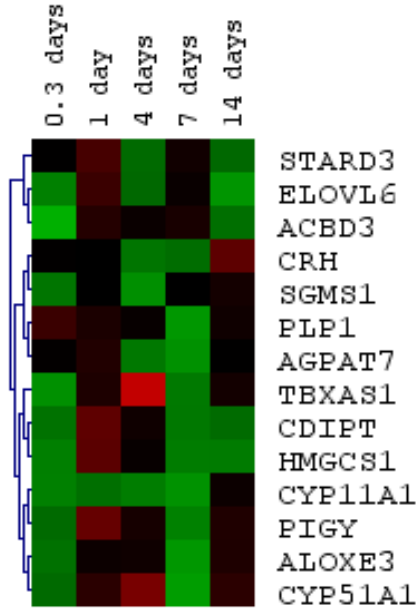

Cell-fate commitment

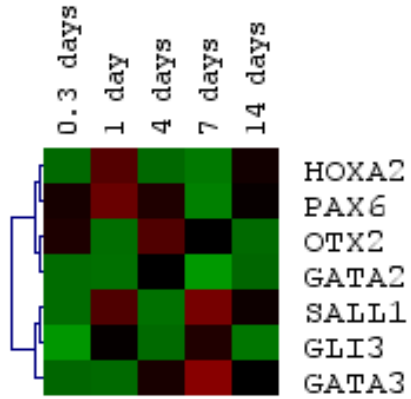

Zheng et al. (2010) BMC Genomics 11:553

Transcription factor binding site bias analysis

For all regulated genes at each time-point, download DNA sequence 500bp and 2000bp upstream of ATG

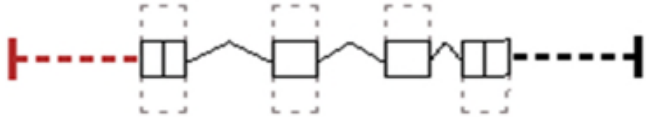

List regulated genes with GO:0003700 'transcription factor activity'

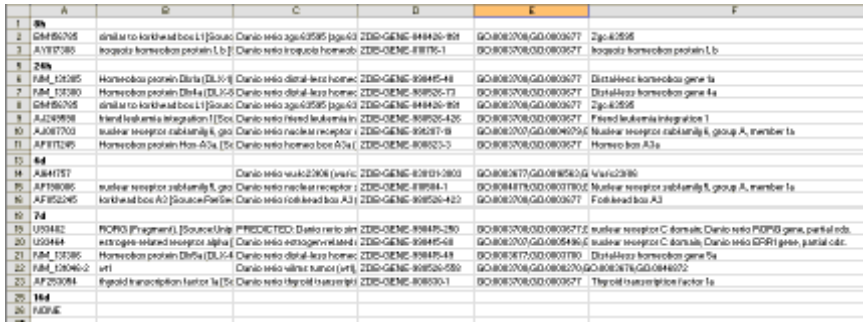

Analyse sequences for presence of all Transcription Factor Binding Sites (TFBS) in the Transfac (2005) database using the 'findpattern' routine of the GCG Wisconsin Package.

TRANSFAC
the gene regulation databases

Filter list for regulated TF

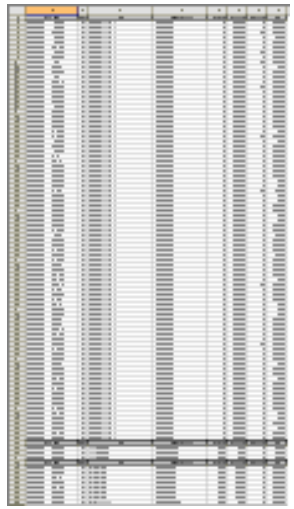

Count number of genes with TFBS to each regulated TF and calculate the percentage of regulated genes with TFBS to regulated TF.

Zheng et al. (2010) BMC Genomics 11:553

Frequency of transcription factor binding sites (TFBS) in regulated genes to regulated transcription factors (TFs)

Hypothesis: If expression of TF influences expression of genes, then, the proportion of regulated genes with TFBS to a regulated TF should change over time and with Zn status.

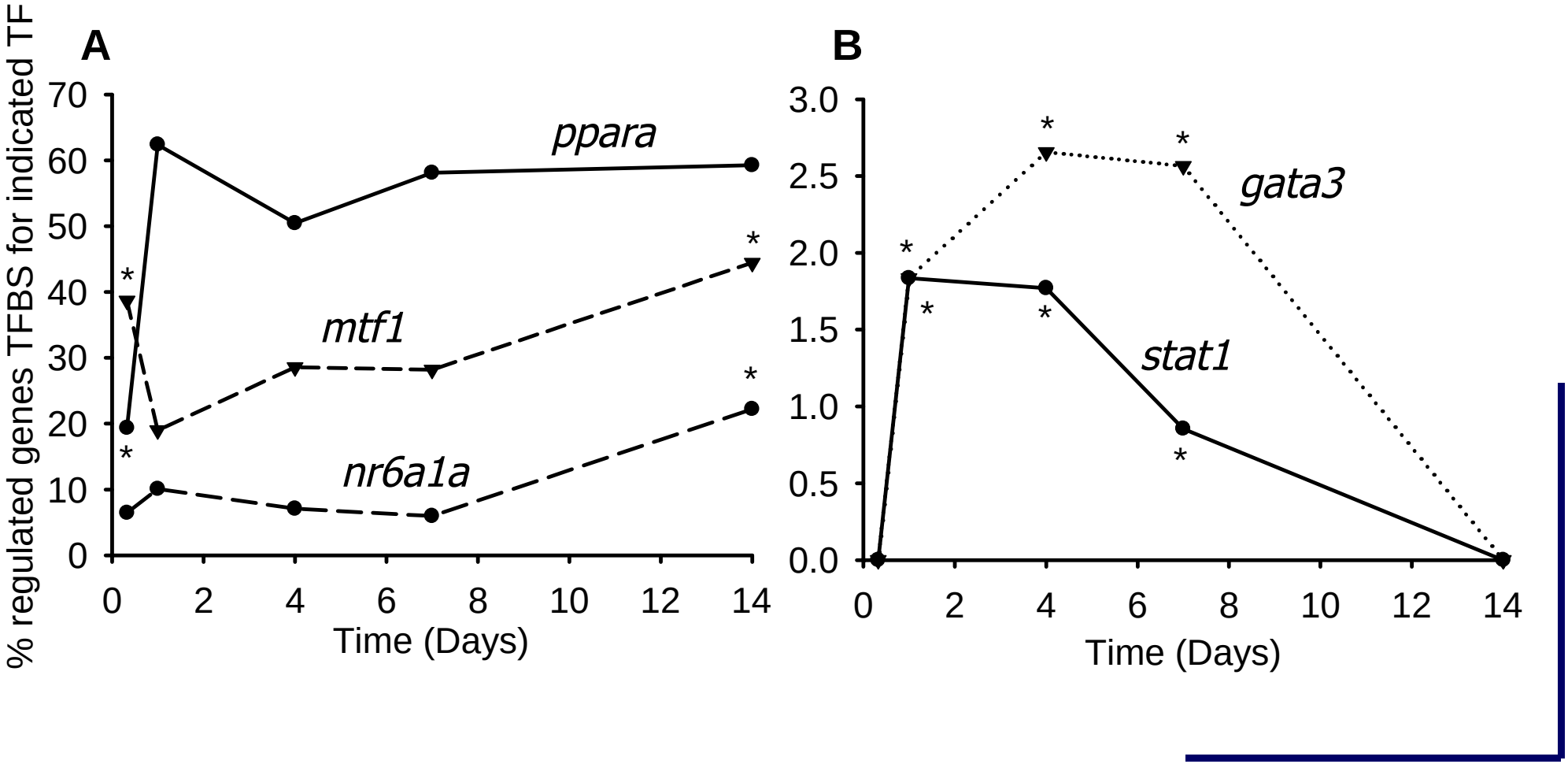

Zheng et al. (2010) BMC Genomics 11:553

Zinc regulatory pathways during zinc exposure

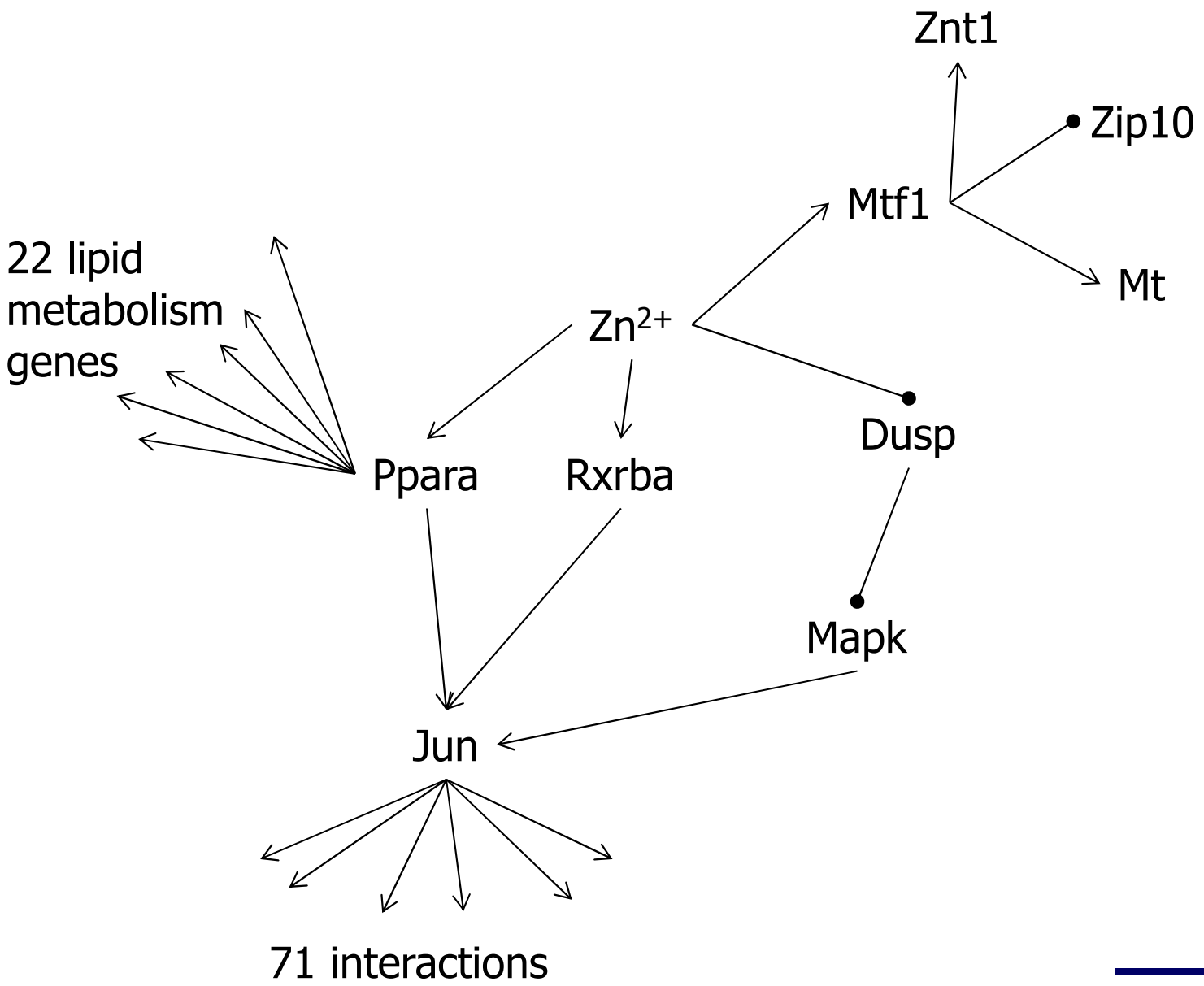

Hogstrand 2011 in: Fish Physiology, Vol. 31, Part A, pp 135-200

Zinc induces ER stress and UPR up-regulated lipolysis via the activation of cAMP/PKA signalling pathway

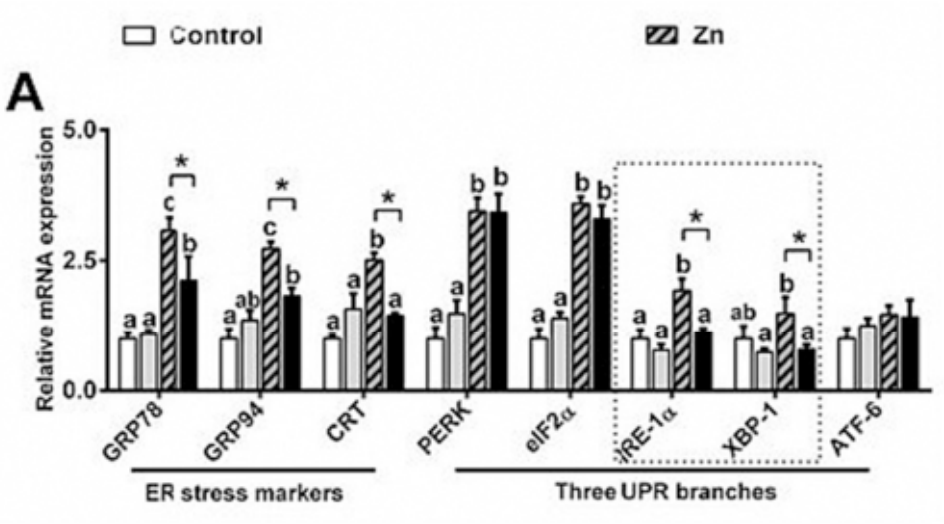

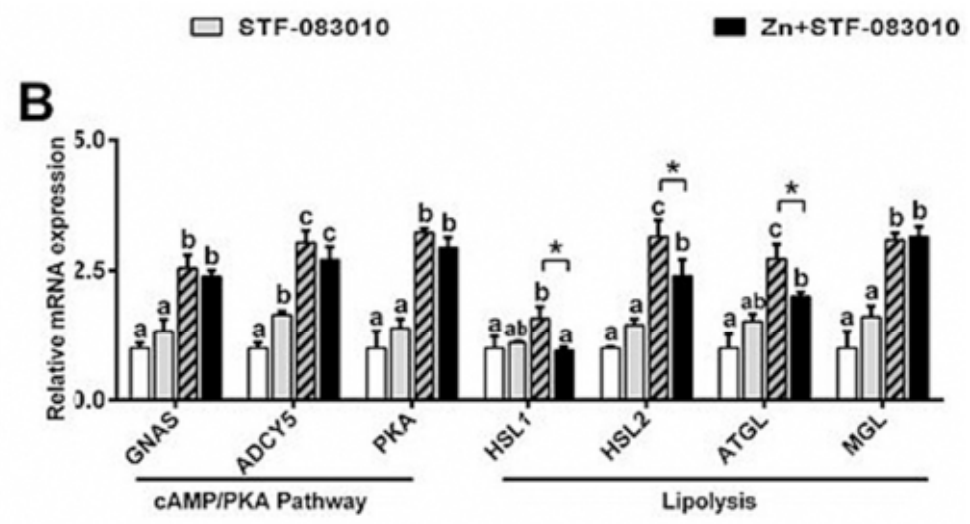

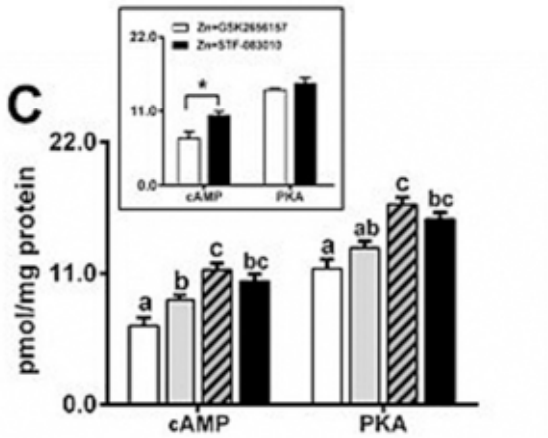

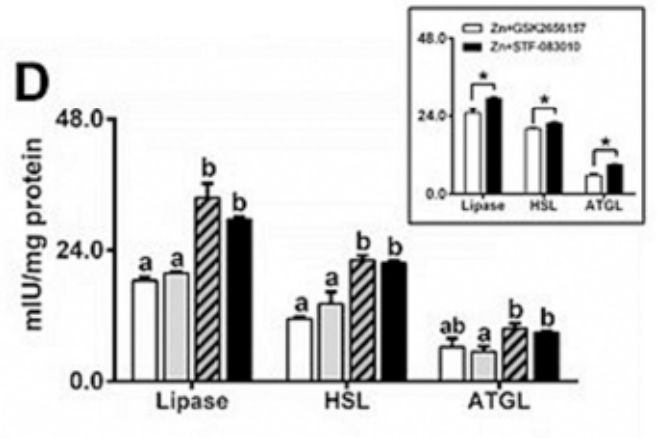

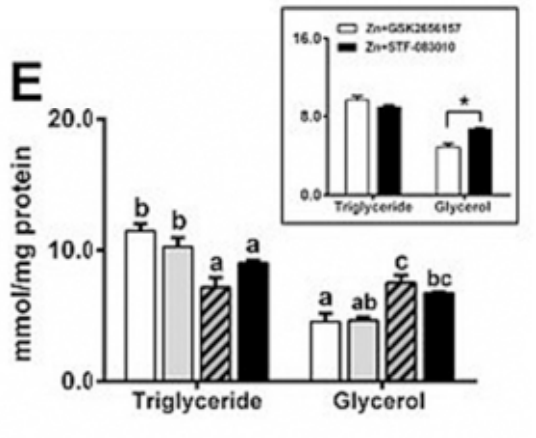

Song et al. 2017 Environ Pollut 228:256-264

Zinc exposure stimulates IP3 and RyR dependent Ca^{2+} release from the ER

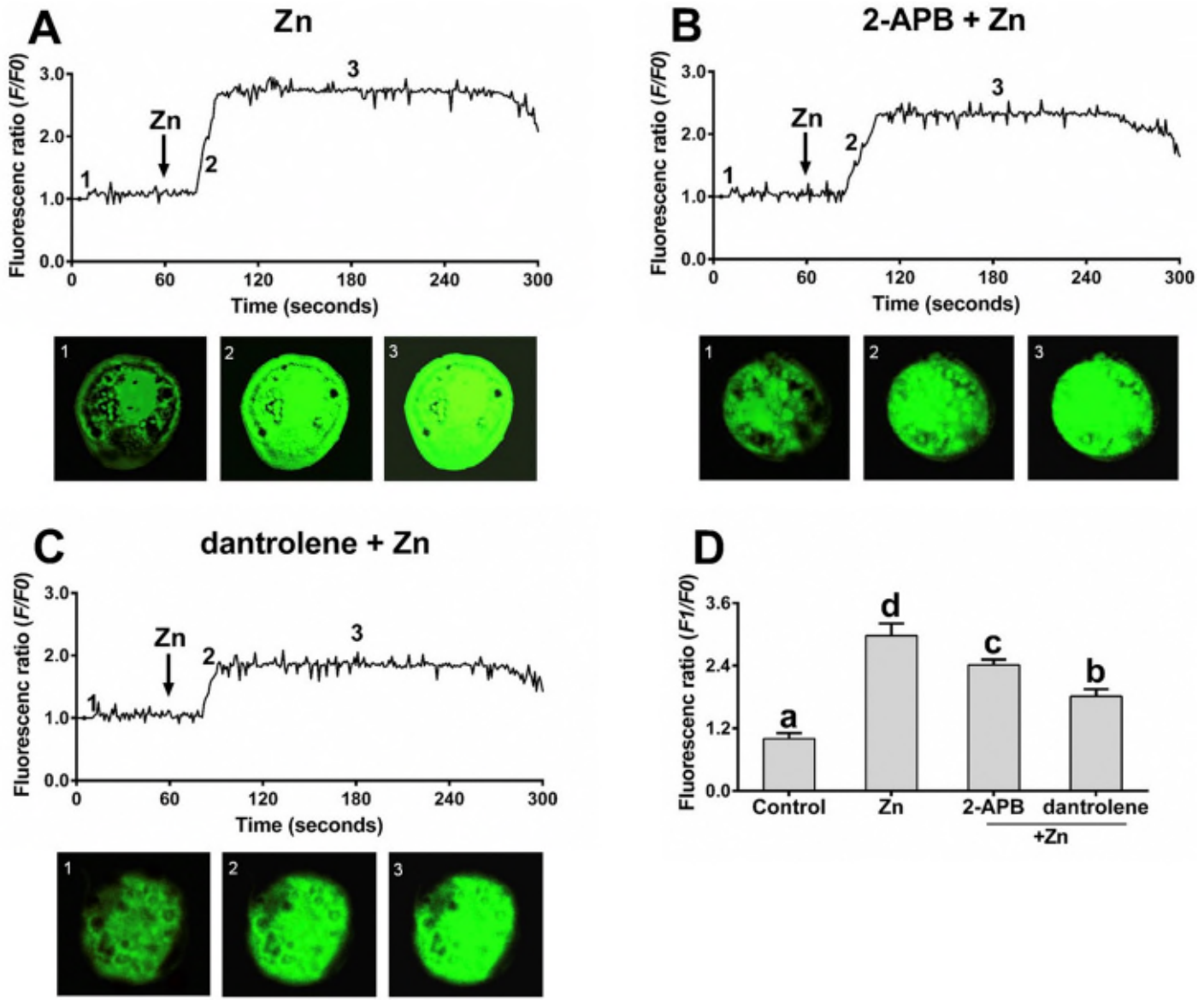

Song et al. 2017 Environ Pollut 228:256-264

Pathway resulting in lipolysis during zinc exposure

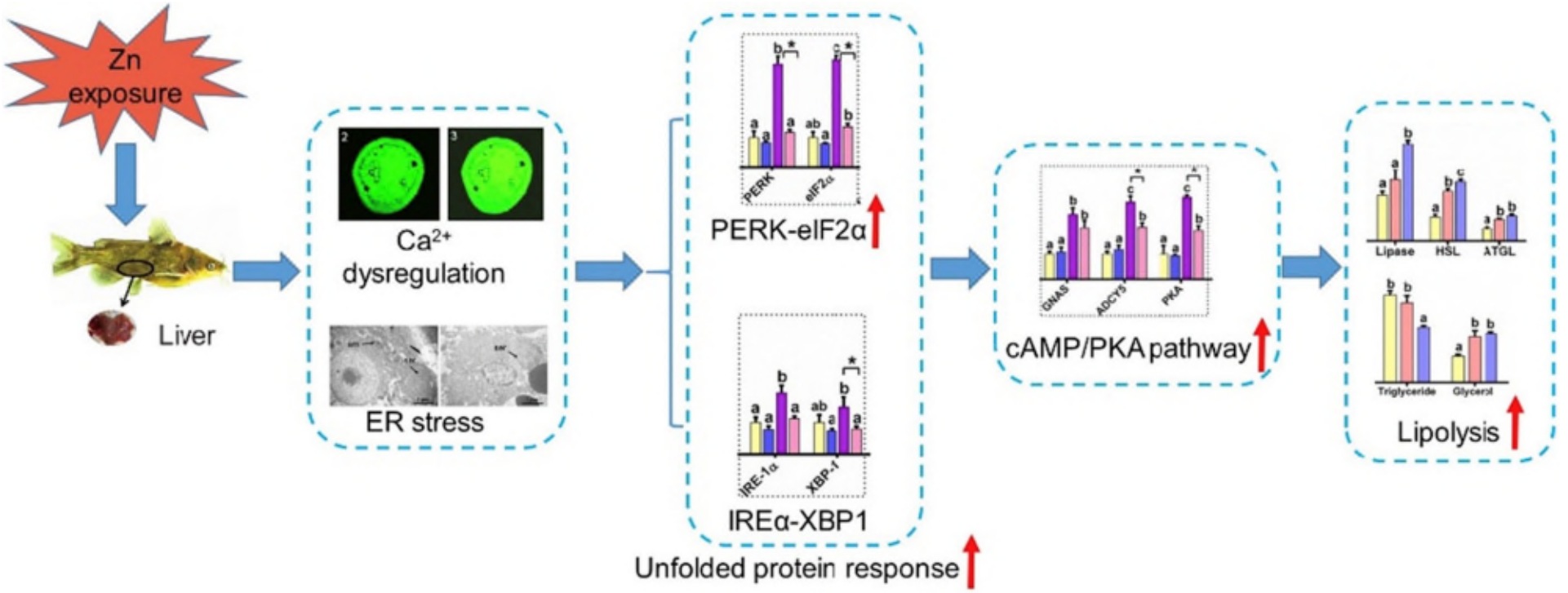

Song et al. 2017 Environ Pollut 228:256-264

Dietary zinc reduces triacyl glycerol content in the yellow catfish intestine

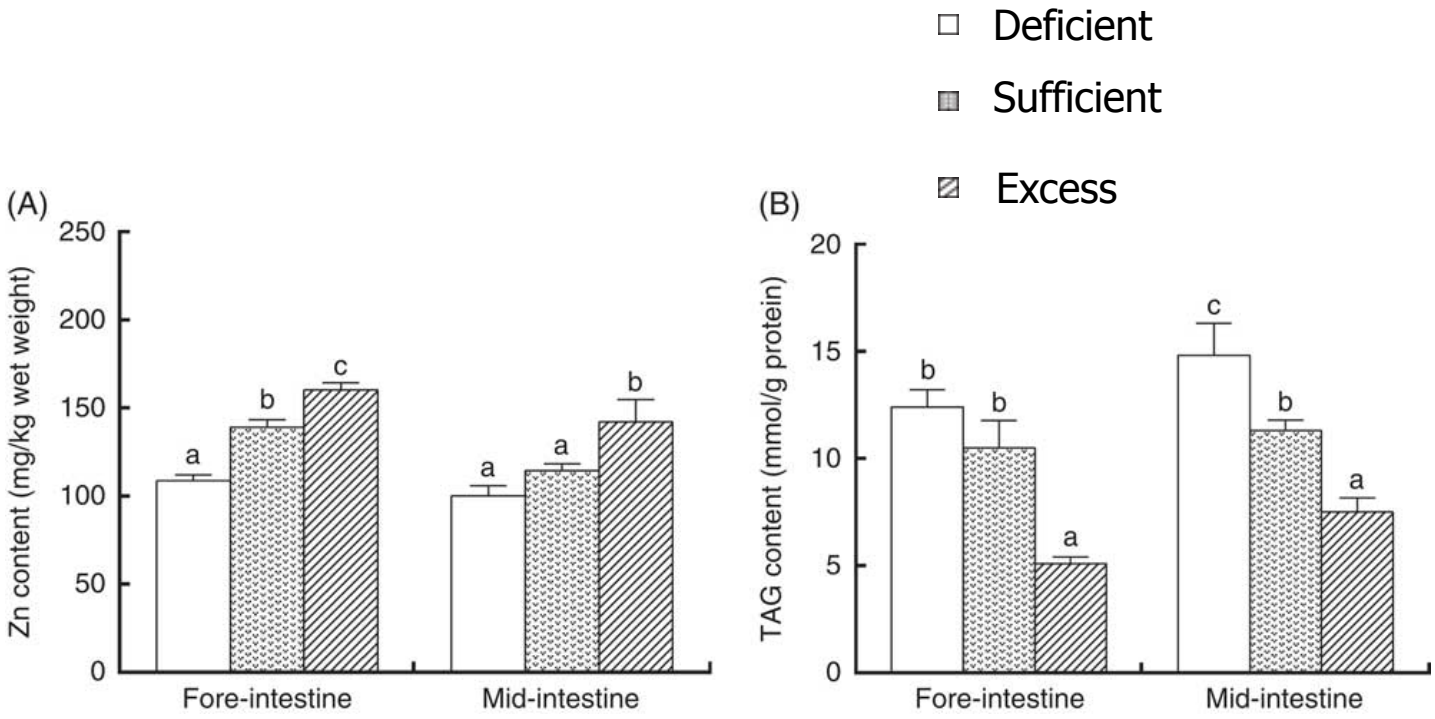

Chen et al. 2017 Br J Nutr. 2017 118(8):570-579

Identifying Health Impacts of Exposure to Copper Using Transcriptomics and Metabolomics in a Fish Model

EDUARDA M. SANTOS,*,† JONATHAN S. BALL,† TIM D. WILLIAMS,‡ HUIFENG WU,‡ FERNANDO ORTEGA,‡ RONNY VAN AERLE,† IOANNA KATSIADAKI,§ FRANCESCO FALCIANI,‡ MARK R. VIANT,‡ JAMES K. CHIPMAN,‡ AND CHARLES R. TYLER†

Exposure of male sticklebacks to 128µg Cu/L
Present study

Mouse model of Wilson's disease (ATP7B -/-)
(Huster et al., 2007)

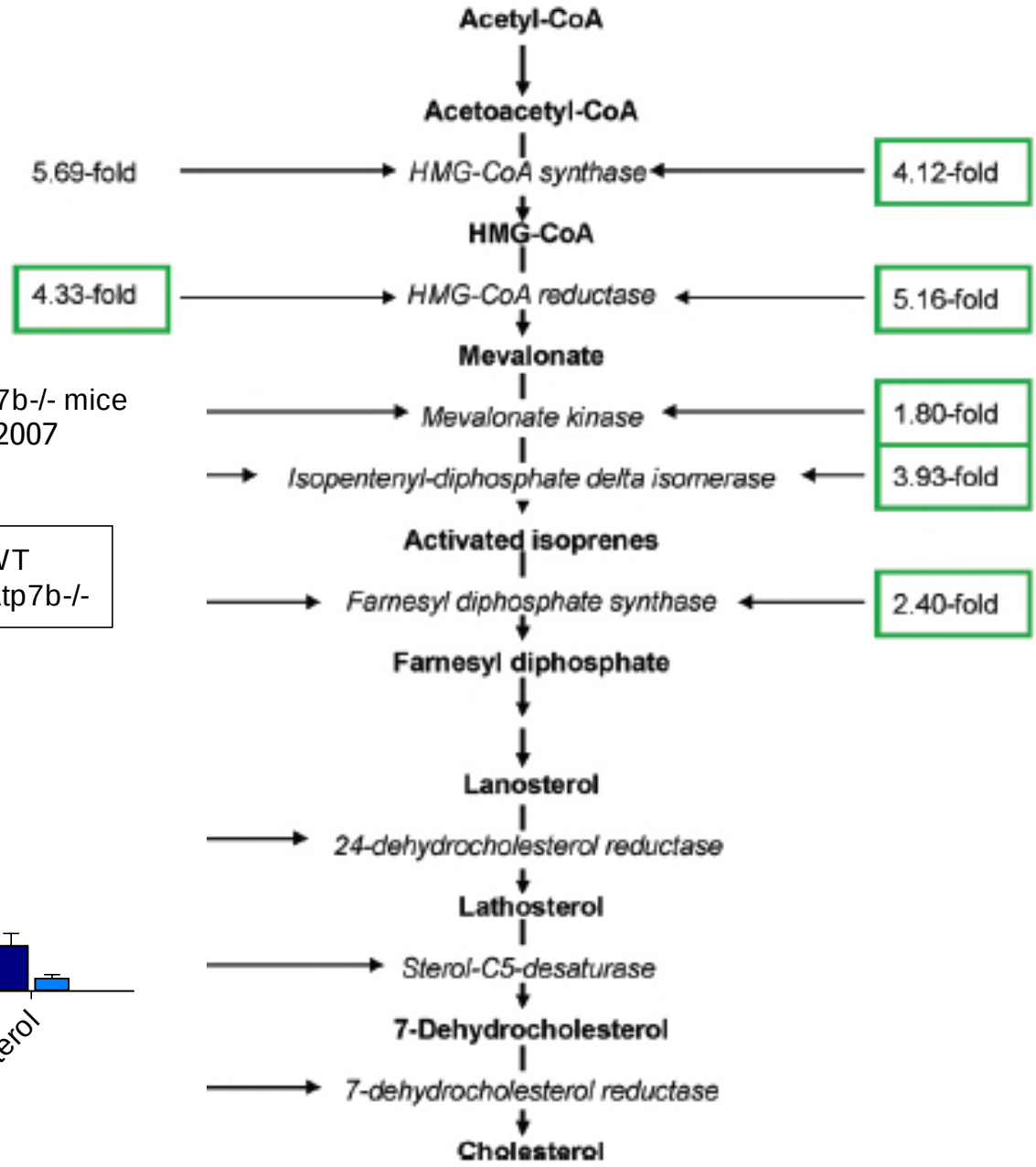

Serum lipids in the 6-week-old control and Atp7b-/- mice
Huster et al., J BIOL CHEM 282: 8343–8355, 2007

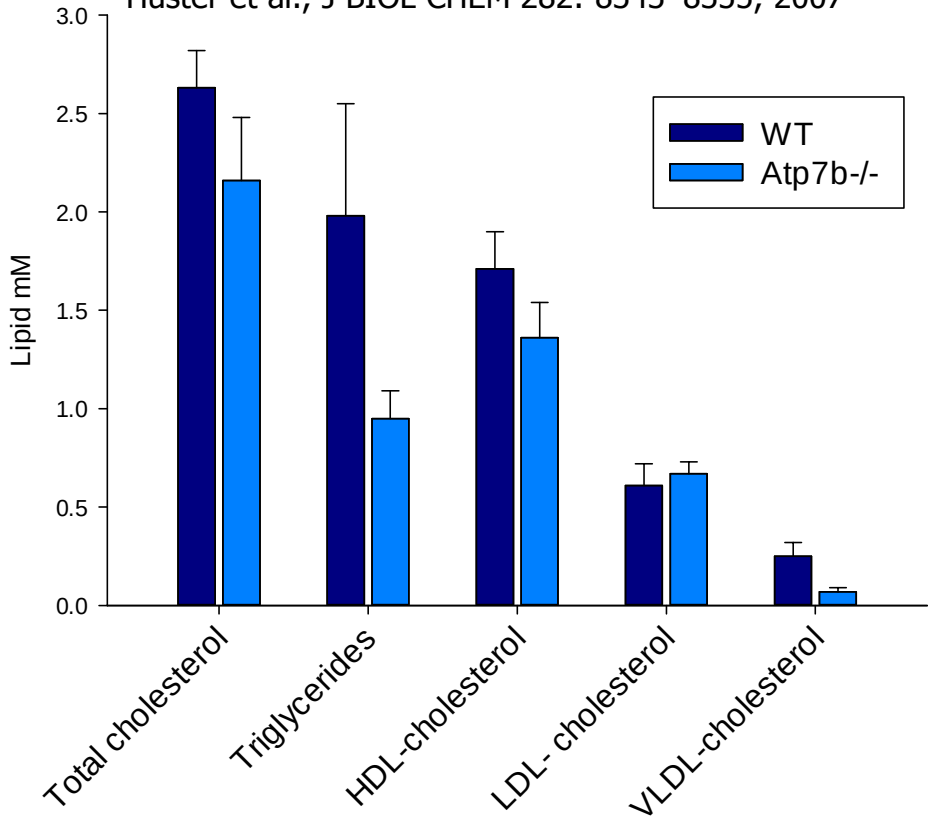

Environ. Sci. Technol. **2010**, *44*, 820–826

Yadetie et al. BMC Genomics 2014, 15:481
http://www.biomedcentral.com/1471-2164/15/481

BMC Genomics

RESEARCH ARTICLE Open Access

Liver transcriptome analysis of Atlantic cod (*Gadus morhua*) exposed to PCB 153 indicates effects on cell cycle regulation and lipid metabolism

Fekadu Yadetie[1,2*], Odd André Karlsen[1,2], Marta Eide[2], Christer Hogstrand[3] and Anders Goksøyr[2]

SCAP/SREBP Transcriptional Control of Cholesterol and FA Biosynthesis

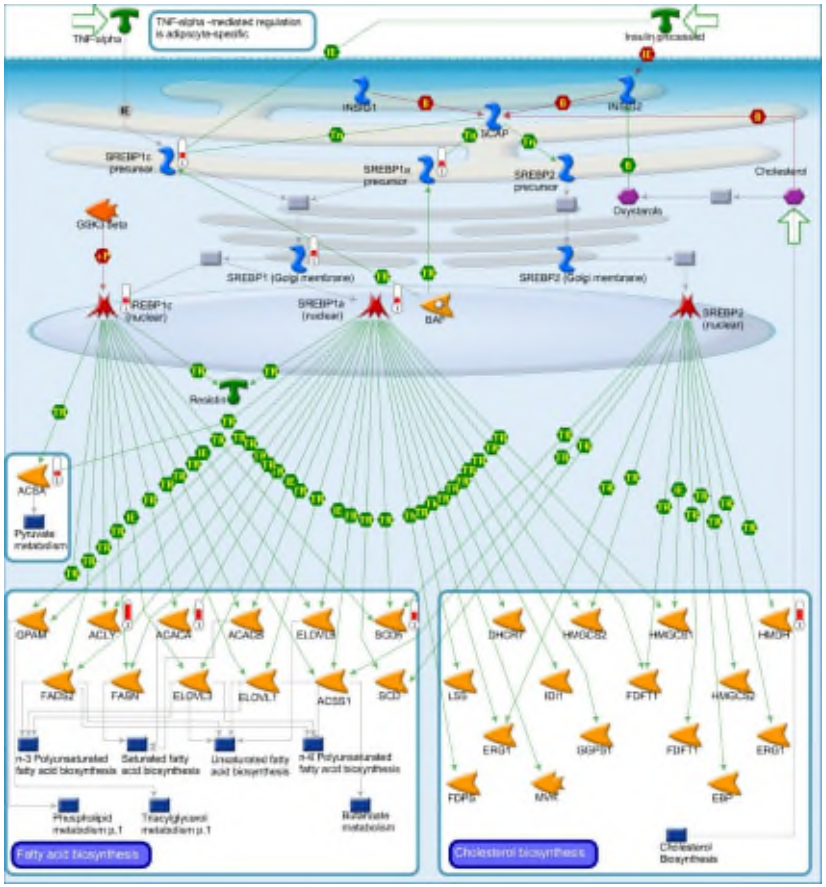

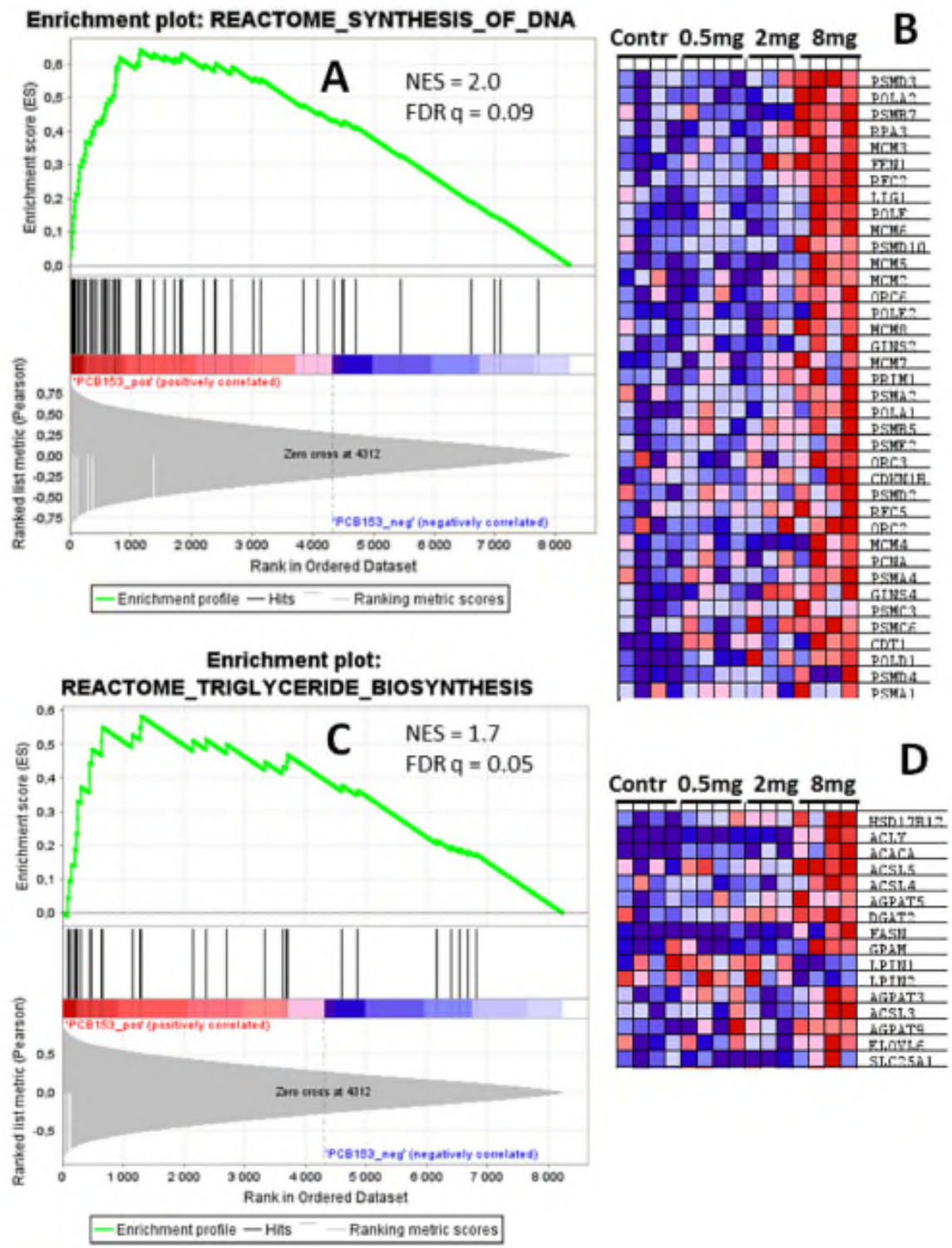

Yadetie et al. 2014 *BMC*

Li et al. BMC Systems Biology 2011, 5:63
http://www.biomedcentral.com/1752-0509/5/63

BMC Systems Biology

RESEARCH ARTICLE Open Access

A computational model of the hypothalamic - pituitary - gonadal axis in female fathead minnows (*Pimephales promelas*) exposed to 17α-ethynylestradiol and 17β-trenbolone

Zhenhong Li[1], Kevin J Kroll[2], Kathleen M Jensen[3], Daniel L Villeneuve[3], Gerald T Ankley[3], Jayne V Brian[4], María S Sepúlveda[5], Edward F Orlando[6], James M Lazorchak[7], Mitchell Kostich[7], Brandon Armstrong[8], Nancy D Denslow[2] and Karen H Watanabe[1*]

Abstract

Background: Endocrine disrupting chemicals (e.g., estrogens, androgens and their mimics) are known to affect reproduction in fish. 17α-ethynylestradiol is a synthetic estrogen used in birth control pills. 17β-trenbolone is a relatively stable metabolite of trenbolone acetate, a synthetic androgen used as a growth promoter in livestock. Both 17α-ethynylestradiol and 17β-trenbolone have been found in the aquatic environment and affect fish reproduction. In this study, we developed a physiologically-based computational model for female fathead minnows (FHM, *Pimephales promelas*), a small fish species used in ecotoxicology, to simulate how estrogens (i.e., 17α-ethynylestradiol) or androgens (i.e., 17β-trenbolone) affect reproductive endpoints such as plasma concentrations of steroid hormones (e.g., 17β-estradiol and testosterone) and vitellogenin (a precursor to egg yolk proteins).

Results: Using Markov Chain Monte Carlo simulations, the model was calibrated with data from unexposed, 17α-ethynylestradiol-exposed, and 17β-trenbolone-exposed FHMs. Four Markov chains were simulated, and the chains for each calibrated model parameter (26 in total) converged within 20,000 iterations. With the converged parameter values, we evaluated the model's predictive ability by simulating a variety of independent experimental data. The model predictions agreed with the experimental data well.

Conclusions: The physiologically-based computational model represents the hypothalamic-pituitary-gonadal axis in adult female FHM robustly. The model is useful to estimate how estrogens (e.g., 17α-ethynylestradiol) or androgens (e.g., 17β-trenbolone) affect plasma concentrations of 17β-estradiol, testosterone and vitellogenin, which are

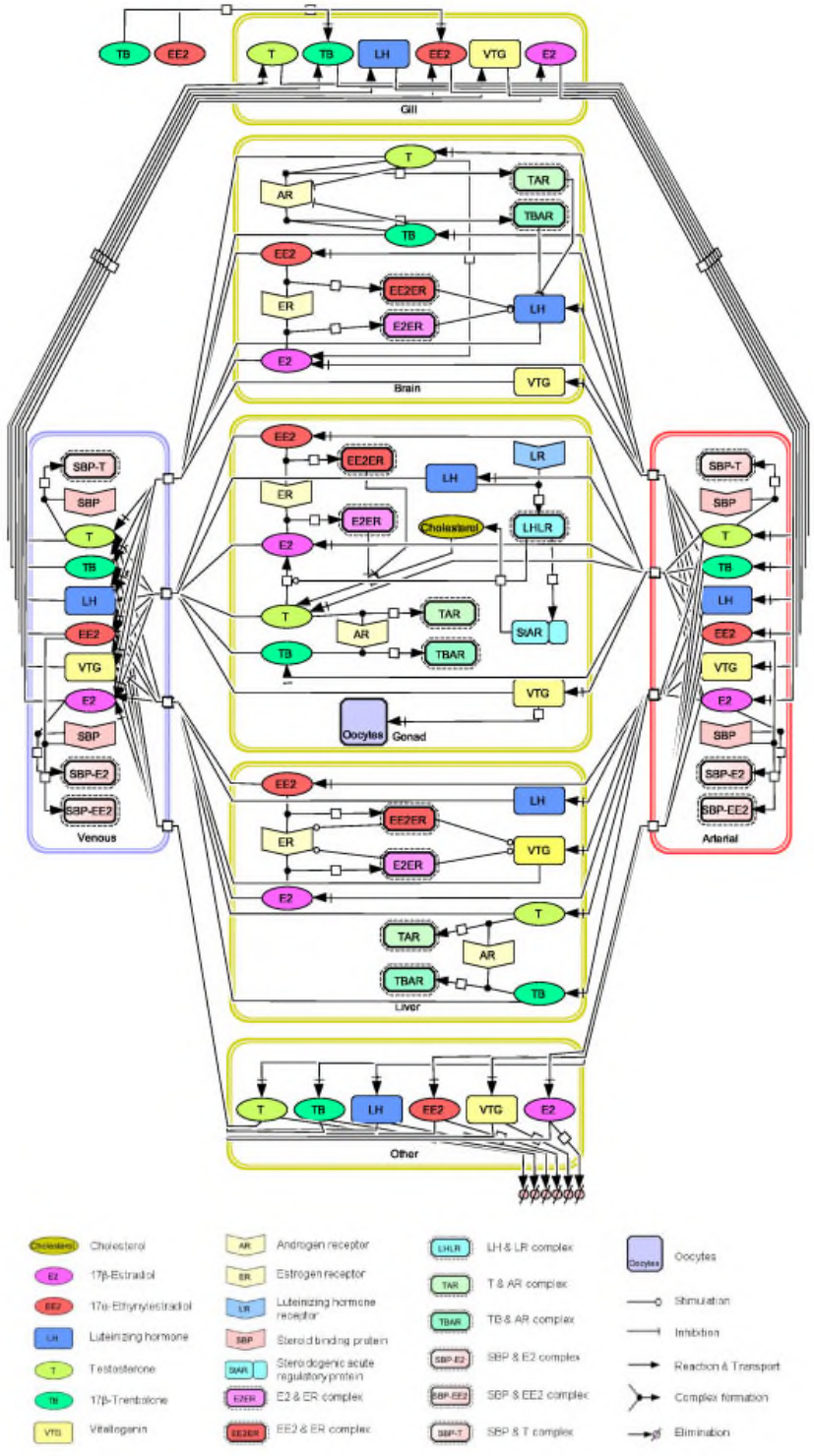

Gonad

$$\frac{d(C_{\mathrm{LHLR,gon}})}{dt} = k_{\mathrm{1\_LHLR,gon}} C_{\mathrm{LH,gon}} C_{\mathrm{LR,gon}} - K_{\mathrm{d\_LHLR,gon}} k_{\mathrm{1\_LHLR,gon}} C_{\mathrm{LHLR,gon}} \quad \text{(Equation 1)}$$

$$\frac{d(C_{\mathrm{TAR,gon}})}{dt} = k_{\mathrm{1\_TAR,gon}} C_{\mathrm{T,gon}} C_{\mathrm{AR,gon}} - K_{\mathrm{d\_TAR,gon}} k_{\mathrm{1\_TAR,gon}} C_{\mathrm{TAR,gon}} \quad \text{(Equation 1)}$$

$$\frac{d(C_{\mathrm{E2ER,gon}})}{dt} = k_{\mathrm{1\_E2ER,gon}} C_{\mathrm{E2,gon}} C_{\mathrm{ER,gon}} - K_{\mathrm{d\_E2ER,gon}} k_{\mathrm{1\_E2ER,gon}} C_{\mathrm{E2ER,gon}} \quad \text{(Equation 1)}$$

$$\frac{d(C_{\mathrm{TBAR,gon}})}{dt} = k_{\mathrm{1\_TBAR,gon}} C_{\mathrm{TB,gon}} C_{\mathrm{AR,gon}} - K_{\mathrm{d\_TBAR,gon}} k_{\mathrm{1\_TBAR,gon}} C_{\mathrm{TBAR,gon}} \quad \text{(Equation 1)}$$

$$\frac{d(C_{\mathrm{EE2ER,gon}})}{dt} = k_{\mathrm{1\_EE2ER,gon}} C_{\mathrm{EE2,gon}} C_{\mathrm{ER,gon}} - K_{\mathrm{d\_EE2ER,gon}} k_{\mathrm{1\_EE2ER,gon}} C_{\mathrm{EE2ER,gon}} \quad \text{(Equation 1)}$$

$$\frac{d(C_{\mathrm{LH,gon}} V_{\mathrm{gon}})}{dt} = F_{\mathrm{gon}} (\mathrm{CArt}_{\mathrm{LH}} - \frac{C_{\mathrm{LH,gon}}}{\lambda_{\mathrm{LH,gon}}}) - V_{\mathrm{gon}} (k_{\mathrm{1\_LHLR,gon}} C_{\mathrm{LH,gon}} C_{\mathrm{LR,gon}} - K_{\mathrm{d\_LHLR,gon}} k_{\mathrm{1\_LHLR,gon}} C_{\mathrm{LHLR,gon}})$$

$$\frac{d(C_{\mathrm{T,gon}} V_{\mathrm{gon}})}{dt} = F_{\mathrm{gon}} (\mathrm{CArt}_{\mathrm{T}} - \frac{C_{\mathrm{T,gon}}}{\lambda_{\mathrm{T,gon}}}) - \frac{k_{\mathrm{E2\_LHLR,gon}} C_{\mathrm{LHLR,gon}} \mathrm{Vmax}_{\mathrm{aro,gon}} C_{\mathrm{T,gon}}}{\mathrm{Km}_{\mathrm{aro,gon}} + C_{\mathrm{T,gon}}}$$
$$+ \frac{\mathrm{Vmax}_{\mathrm{Scc,gon}} C_{\mathrm{Chol,gon}}^{n_{\mathrm{T}}}}{\mathrm{K}_{0.5\mathrm{Scc,gon}}^{n_{\mathrm{T}}} + C_{\mathrm{Chol,gon}}^{n_{\mathrm{T}}}} \div (1 + \frac{C_{\mathrm{E2ER,gon}} + C_{\mathrm{EE2ER,gon}}}{K_{\mathrm{T}}})$$
$$- V_{\mathrm{gon}} (k_{\mathrm{1\_TAR,gon}} C_{\mathrm{T,gon}} C_{\mathrm{AR,gon}} - K_{\mathrm{d\_TAR,gon}} k_{\mathrm{1\_TAR,gon}} C_{\mathrm{TAR,gon}})$$

$$\frac{d(C_{\mathrm{Vtg,gon}} V_{\mathrm{gon}})}{dt} = F_{\mathrm{gon}} (\mathrm{CArt}_{\mathrm{Vtg}} - \frac{C_{\mathrm{Vtg,gon}}}{\lambda_{\mathrm{Vtg,gon}}}) - k_{\mathrm{VTG,gon}} C_{\mathrm{VTG,gon}} V_{\mathrm{gon}} \quad \text{(Equation 6)}$$

$$\frac{d(C_{\mathrm{E2,gon}} V_{\mathrm{gon}})}{dt} = F_{\mathrm{gon}} (\mathrm{CArt}_{\mathrm{E2}} - \frac{C_{\mathrm{E2,gon}}}{\lambda_{\mathrm{E2,gon}}}) + \frac{\rho_{\mathrm{E2\_LHLR,gon}} C_{\mathrm{LHLR,gon}} \mathrm{Vmax}_{\mathrm{aro,gon}} C_{\mathrm{T,gon}}}{\mathrm{Km}_{\mathrm{aro,gon}} + C_{\mathrm{T,gon}}} \quad \text{(Equation 7)}$$
$$- V_{\mathrm{gon}} (k_{\mathrm{1\_E2ER,gon}} C_{\mathrm{E2,gon}} C_{\mathrm{ER,gon}} - K_{\mathrm{d\_E2ER,gon}} k_{\mathrm{1\_E2ER,gon}} C_{\mathrm{E2ER,gon}})$$

$$\frac{d(C_{\mathrm{TB,gon}} V_{\mathrm{gon}})}{dt} = F_{\mathrm{gon}} (\mathrm{CArt}_{\mathrm{KT}} - \frac{C_{\mathrm{TB,gon}}}{\lambda_{\mathrm{TB,gon}}}) - V_{\mathrm{gon}} (k_{\mathrm{1\_TBAR,gon}} C_{\mathrm{TB,gon}} C_{\mathrm{AR,gon}} - K_{\mathrm{d\_TBAR,gon}} k_{\mathrm{1\_TBAR,gon}} C_{\mathrm{TBAR,gon}})$$

$$\frac{d(C_{\mathrm{EE2,gon}} V_{\mathrm{gon}})}{dt} = F_{\mathrm{gon}} (\mathrm{CArt}_{\mathrm{EE2}} - \frac{C_{\mathrm{EE2,gon}}}{\lambda_{\mathrm{EE2,gon}}}) - V_{\mathrm{gon}} (k_{\mathrm{1\_EE2ER,gon}} C_{\mathrm{EE2,gon}} C_{\mathrm{ER,gon}} - K_{\mathrm{d\_EE2ER,gon}} k_{\mathrm{1\_EE2ER,gon}} C_{\mathrm{EE2ER,g}}$$

Li et al. BMC Systems Biology 2011, 5:63
http://www.biomedcentral.com/1752-0509/5/63

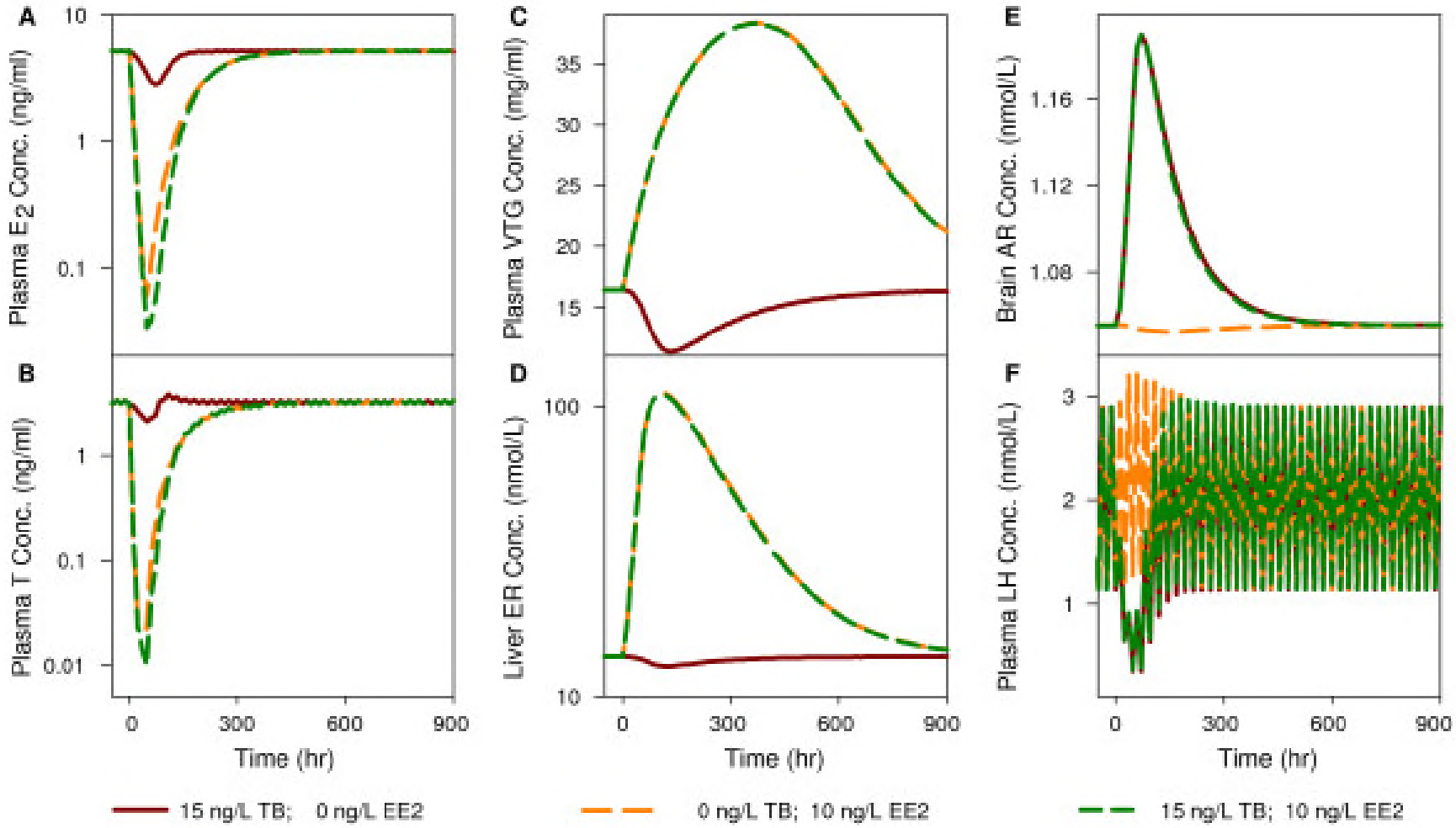

Model predictions for unmeasured reproductive endpoints in female FHMs. The predictions are for female FHMs exposed to 15 ng/L TB, 10 ng/L EE_2, or a mixture of 15 ng/L TB and 10 ng/L EE_2 for 48 hours, respectively: (A) plasma E_2concentration, (B) plasma T concentration, (C) plasma VTG concentration, (D) liver ER concentration, (E) brain AR concentration, and (F) plasma LH conce

Li *et al. BMC Systems Biology* 2011, **5**:63
http://www.biomedcentral.com/1752-0509/5/63

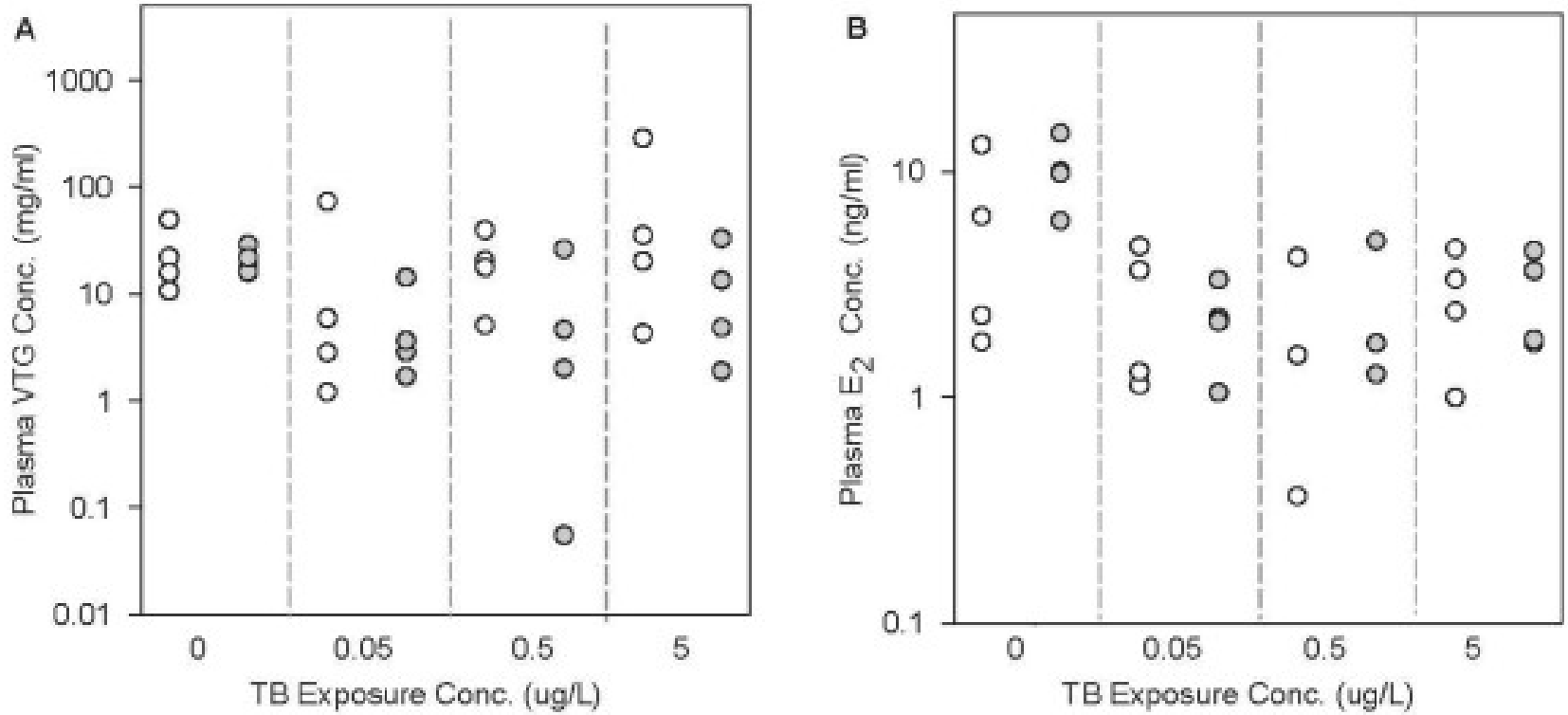

Comparison of model predictions with measured data in female FHMs exposed to TB for 48 hours. *n* = 32. White circles represent model predictions, and grey circles represent measured data

Li *et al. BMC Systems Biology* 2011, **5**:63
http://www.biomedcentral.com/1752-0509/5/63

Relationship of plasma sex steroid concentrations in female fathead minnows to reproductive success and population status

Gerald T. Ankley[a,*], David H. Miller[b], Kathleen M. Jensen[a], Daniel L. Villeneuve[a], Dalma Martinović[a]

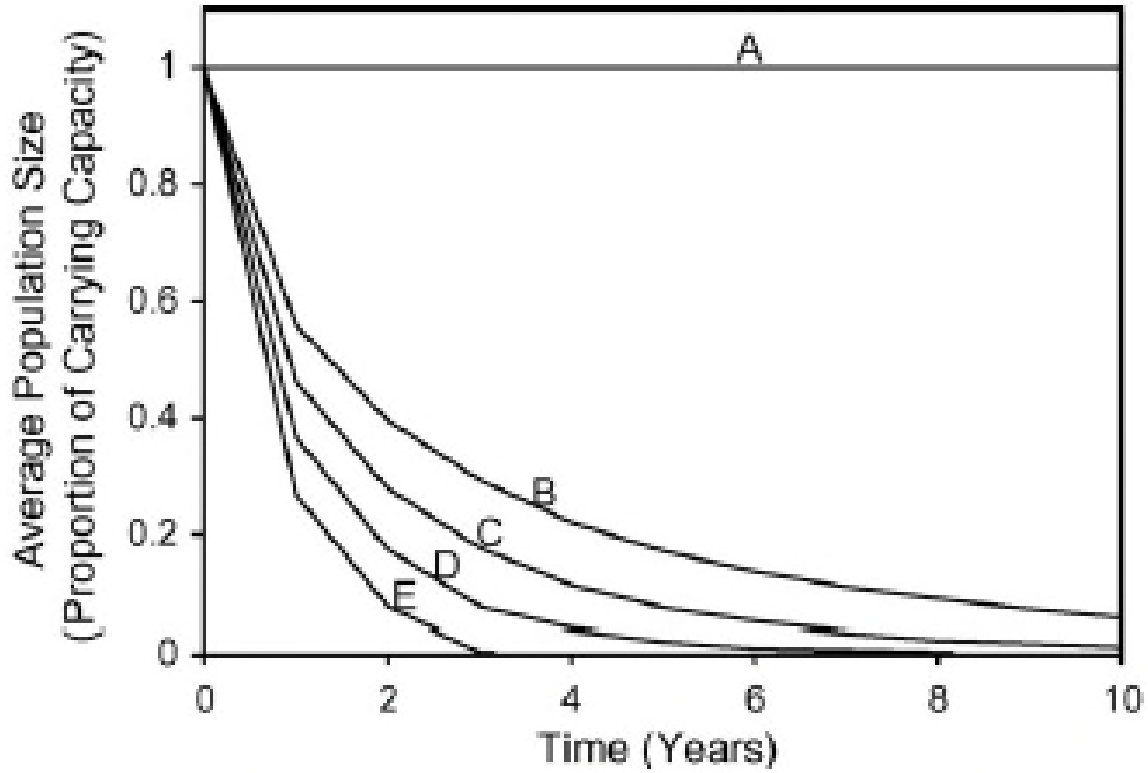

Fig. 4. Relative population trajectories forecasted for a fathead minnow (*Pimephales promelas*) population initially at carrying capacity (baseline conditions) and subsequently exposed to chemicals that depress plasma 17β-estradiol (E2) concentrations. Scenarios illustrated include (A) no reduction in E2, (B) 25% reduction in E2, (C) 50% reduction in E2, (D) 75% reduction in E2, and (E) 100% reduction in E2.

Chemical classification and grouping

Classification through fingerprinting responses

Network-based pipeline for differential connectivity analysis

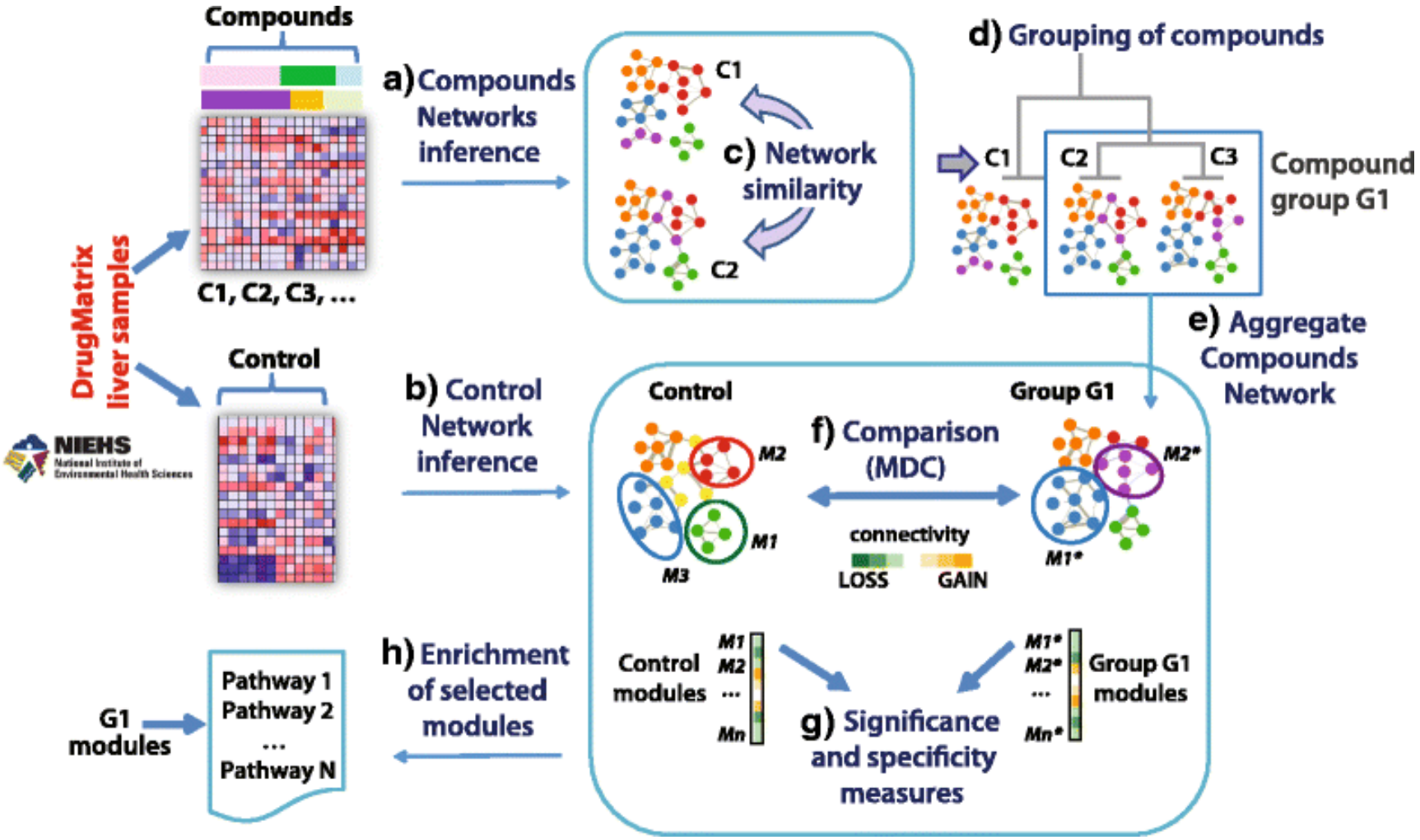

Mulas 2017 BMC Bioinformatics 2017, 18(Suppl 5):130

Similarity-based partial ordering and grouping of chemicals by hierarchical clustering

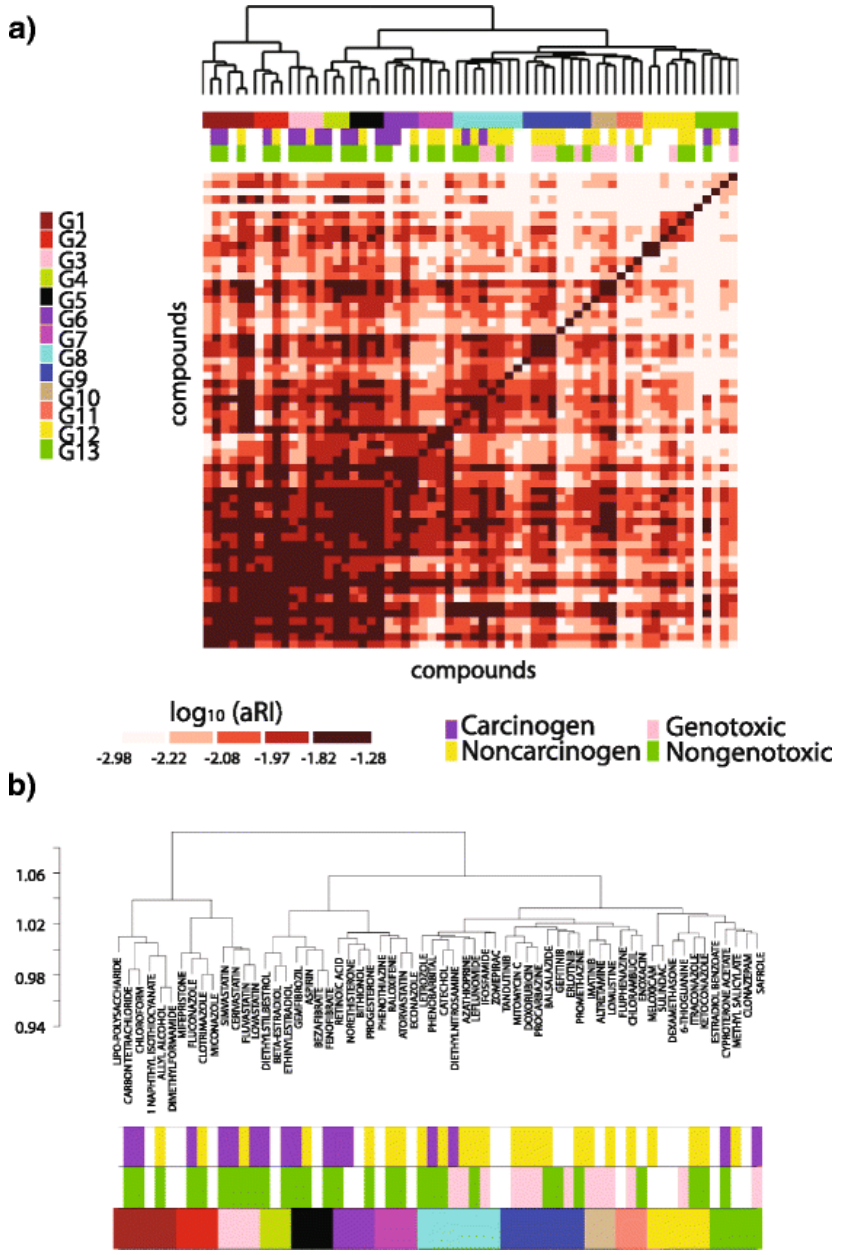

Mulas 2017 BMC Bioinformatics 2017, 18(Suppl 5):130

Chemical connectivity maps: mRNA 'fingerprints' of biological responses to toxicants

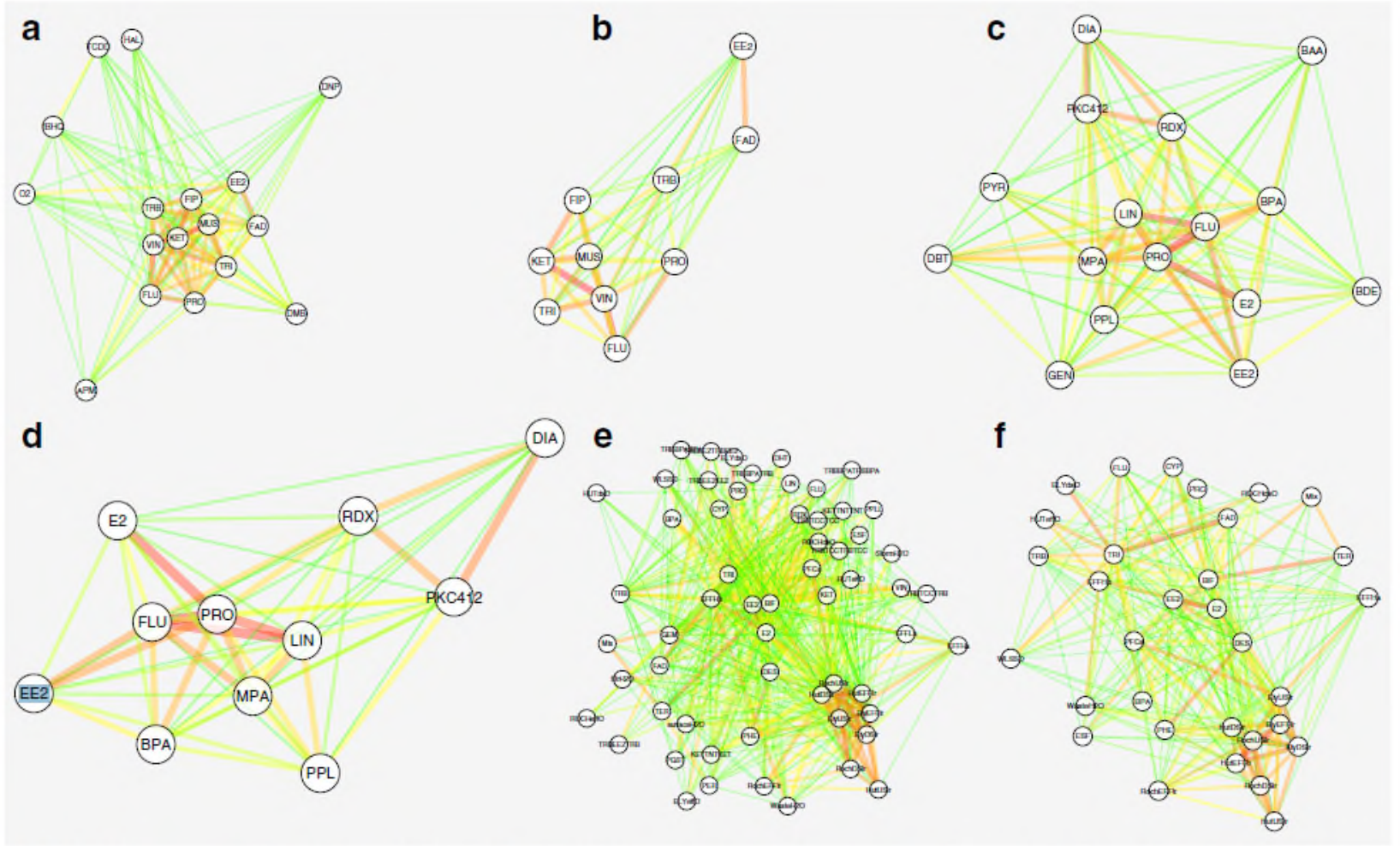

Fig. 1 A network view of chemical-chemical connectivity based on fish samples profiled on various microarray platforms. Each treatment condition is represented as a node. Two nodes are connected by an edge weighted by their connectivity score. A shorter, darker, and wider edge between two nodes denotes a higher connectivity score. All connections shown are statistically significant. **a** ZF 21K: 117 connections among 17 treatment conditions; **b** ZF 21K: 45 connections among 10 nodes with each node containing a connectivity score of ≥ 10 in at least one connection; **c** ZF 43K: 110 connections among 16 treatment conditions; **d** ZF 43K: 54 connections among 11 nodes with each node containing a connectivity score of ≥ 10 in at least one connection; **e** FHM 15K: 541 connections among 53 treatment conditions; **f** FHM 15K: 293 connections among 32 nodes with each node containing a connectivity score of ≥ 10 in at least one connection

Wang et al. BMC Genomics (2016) 17:8

Read-across to estimate different species sensitivities

Creating a predictive framework for DSS

CAS number	Ch
111706	1-
71238	1-
95487	2-
67641	2-
107119	2-
141786	Ac
62533	Be
71432	Be
1E+07	Ca
7487947	M
87865	Pe
105373	Pr
110861	Py
90028	Sa
79016	Tr

noura *erea*
36
.520
10
0300
100
130
64
130
23
0.13
0.38
20
254
1.3
70

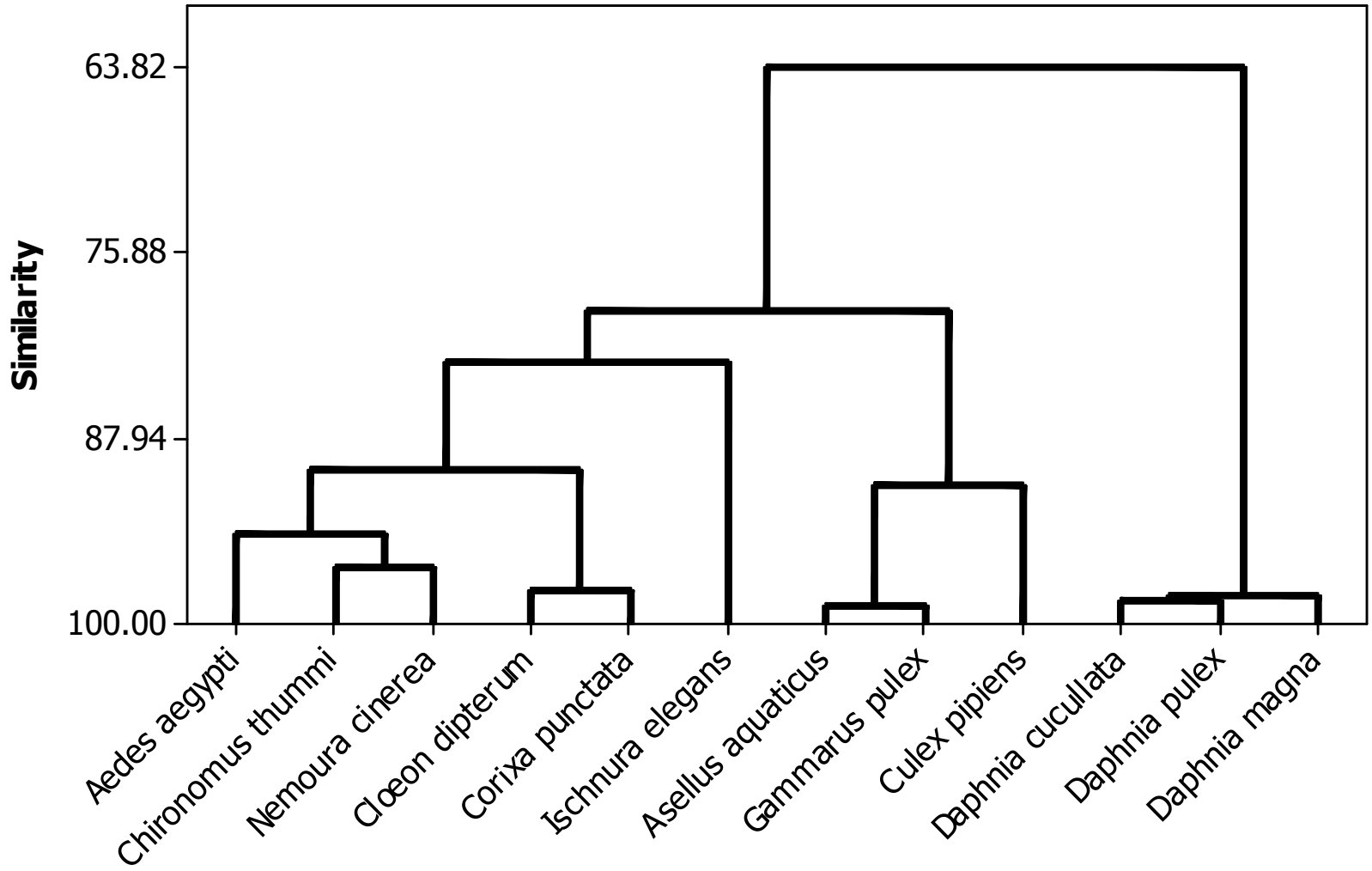

1. **Using toxicity data for phylogenetics**
2. **The distribution in sensitivity is not random**
3. **Related species cluster by sensitivity**

1. Toxicokinetics

External → Internal conc.

2a. Toxicodynamics

Cause of toxicity

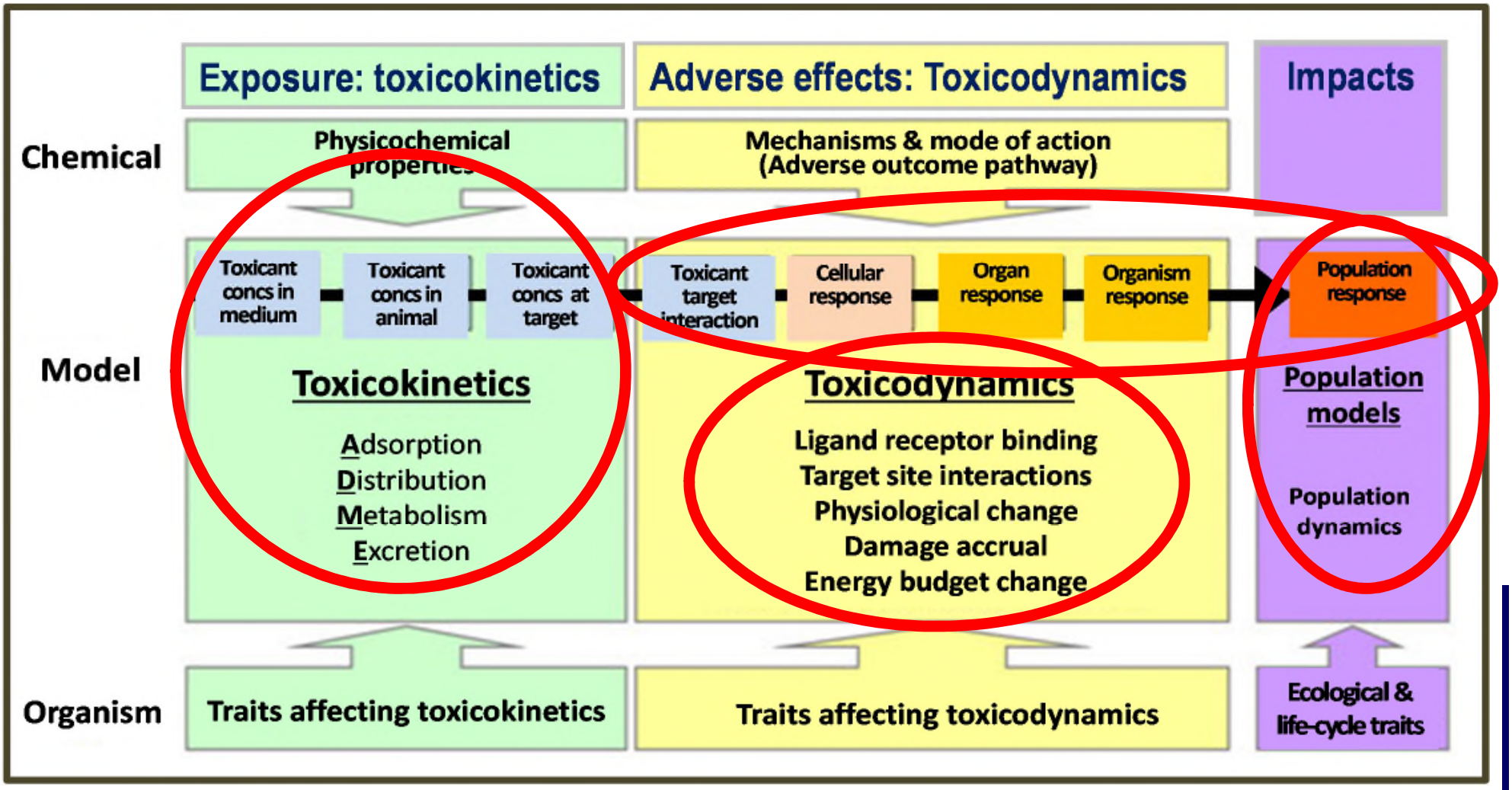

2b. Adverse outcome pathway

Translation to effects

4. Ecological or health effects

Differential toxicant uptake influences internal dose and toxicity

Table 2. Metal body burden and metal-tolerance classification for three taxa found in Big Bayou Creek, Kentucky, USA[a]

Taxon	Metal body burden (μg/g dry weight)[b]				Metal-tolerance classification
	Cadmium	Chromium	Copper	Zinc	
Stenonema spp.	2.04 ± 1.3 (102)	2.47 ± 1.1 (41.2)	28.14 ± 0.9 (1.7)	564.3 ± 6.5 (4.9)	Sensitive
Campostoma anomalum[c]	0.22 ± 0.07 (11)	2.65 ± 0.5 (44.2)	16.8 ± 3.3 (1)	145 ± 15 (1.3)	Intermediate
Cheumatopsyche spp.	0.02 ± 0.01 (1)	0.06 ± 0.01 (1)	24.14 ± 1.8 (1.4)	114.5 ± 4.3 (1)	Tolerant

[a] Body burden measurements were of organisms collected from sampling station BB6 where maximum ecological impact occurred.
[b] Mean ± SD; ratios of metal body burden relative to lowest concentration are given in parentheses for each metal.
[c] Gastrointestinal tract removed.

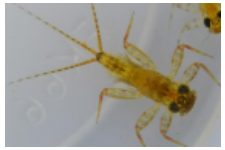

Stenonema sp. (Mayfly)

Campostoma anomalum (Central stoneroller)

Cheumatopsyche sp. (Caddisfly)

Birge et al. 2000 Environ Toxicol Chem. 19(4):1199-1212

Carnivora phylogeny, UGT1A6 mutations, and diet

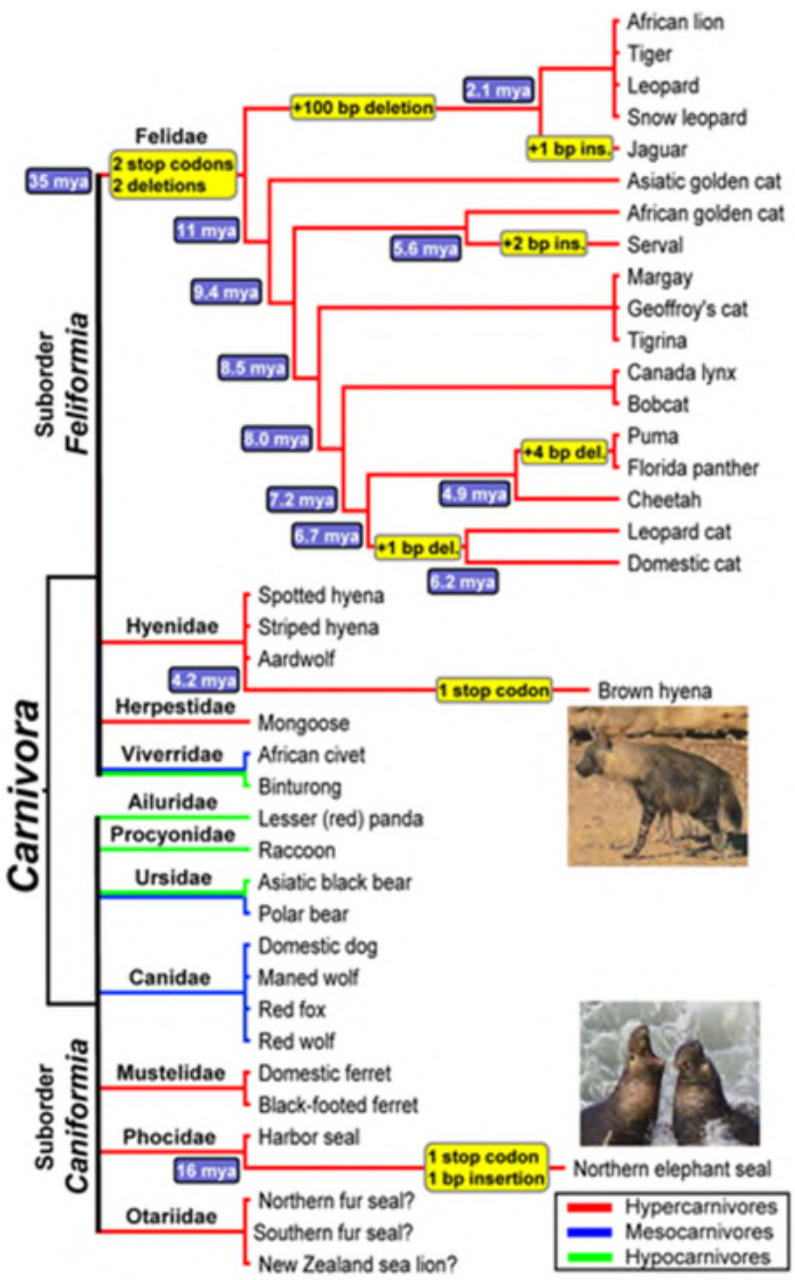

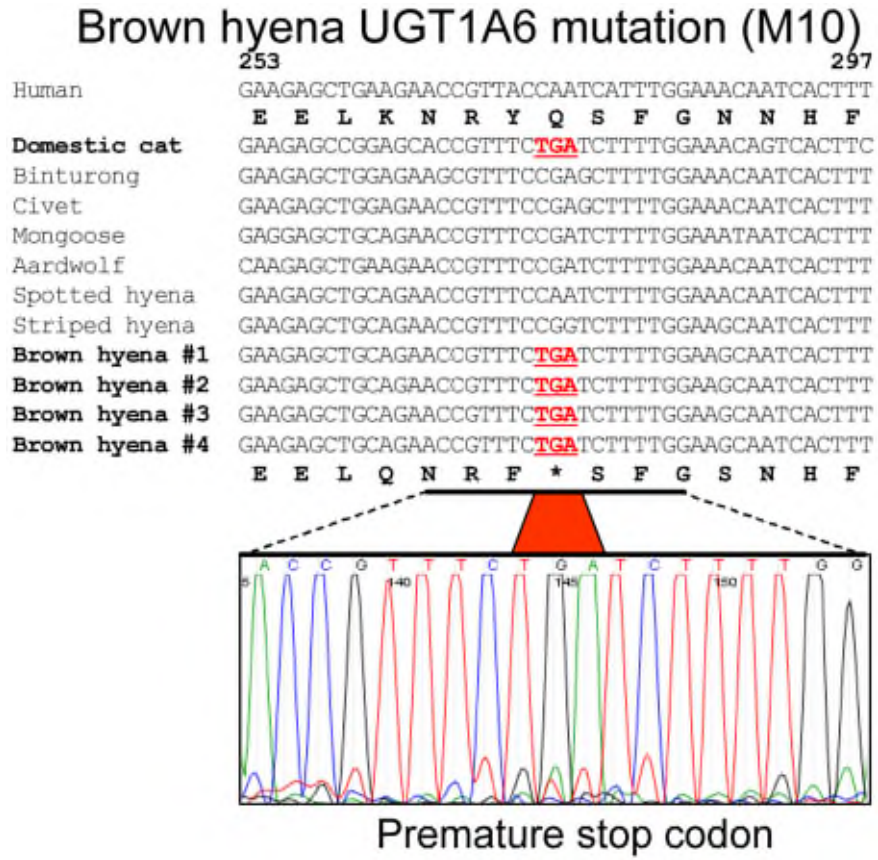

Shrestha et al. 2011 PLoS ONE 6(3): e18046

Species receptor compliment

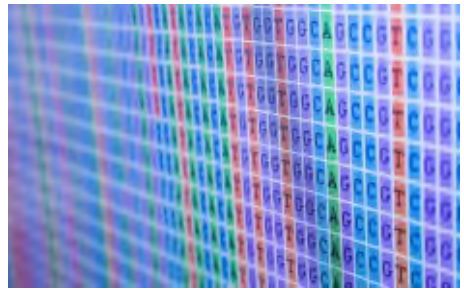

	Ach receptor	Sodium Channel	Neonicotinic
Earthworm	3	2	16
Mollusc	2	3	14
Arthropod	1	1	12
Nematode	2	0	12

Chemical - ligand interactions

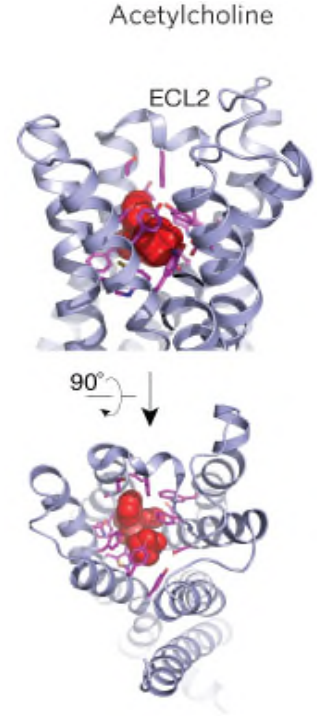

Genome wide ortholog analysis

Bioinformatics

In silico receptor binding studies

Pharmacology and drug discovery

Median similarity and the number of predicted orthologs in all investigated species compared to the human drug targets

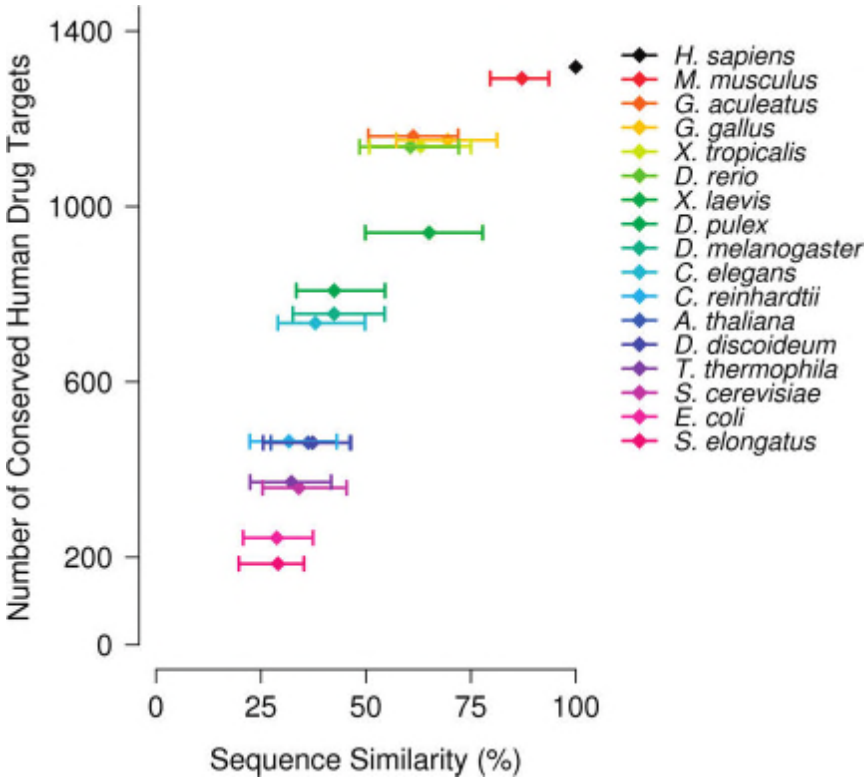

Gunnarsson et al. 2008 ES&T 42:15

Protein sequence similarity across species compared with the bovine androgen receptor (AR)

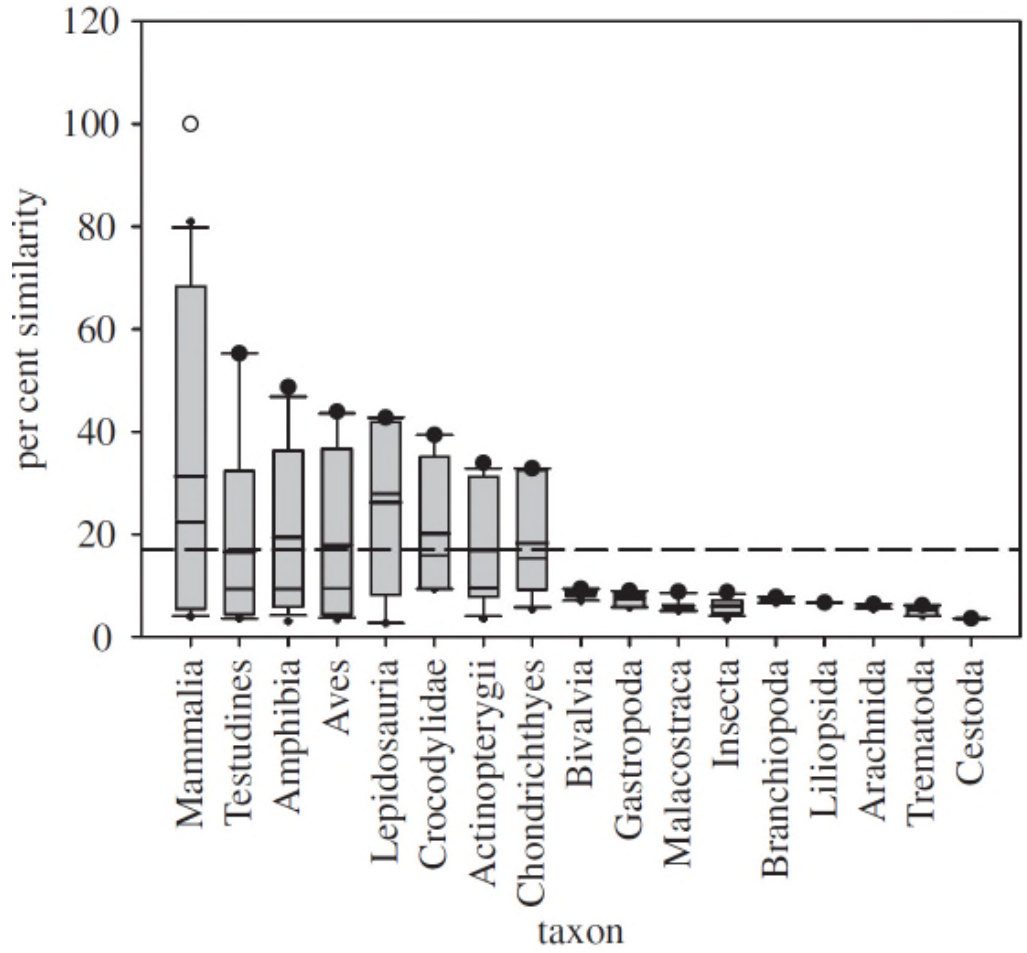

Lalone et al. 2014 Phil. Trans. R. Soc. B 369: 20140022

Community and ecosystem impact (Retrospective monitoring)

Metagenomic profiling, eDNA and aDNA

eDNA – What life discards: A powerful new tool for biological conservation

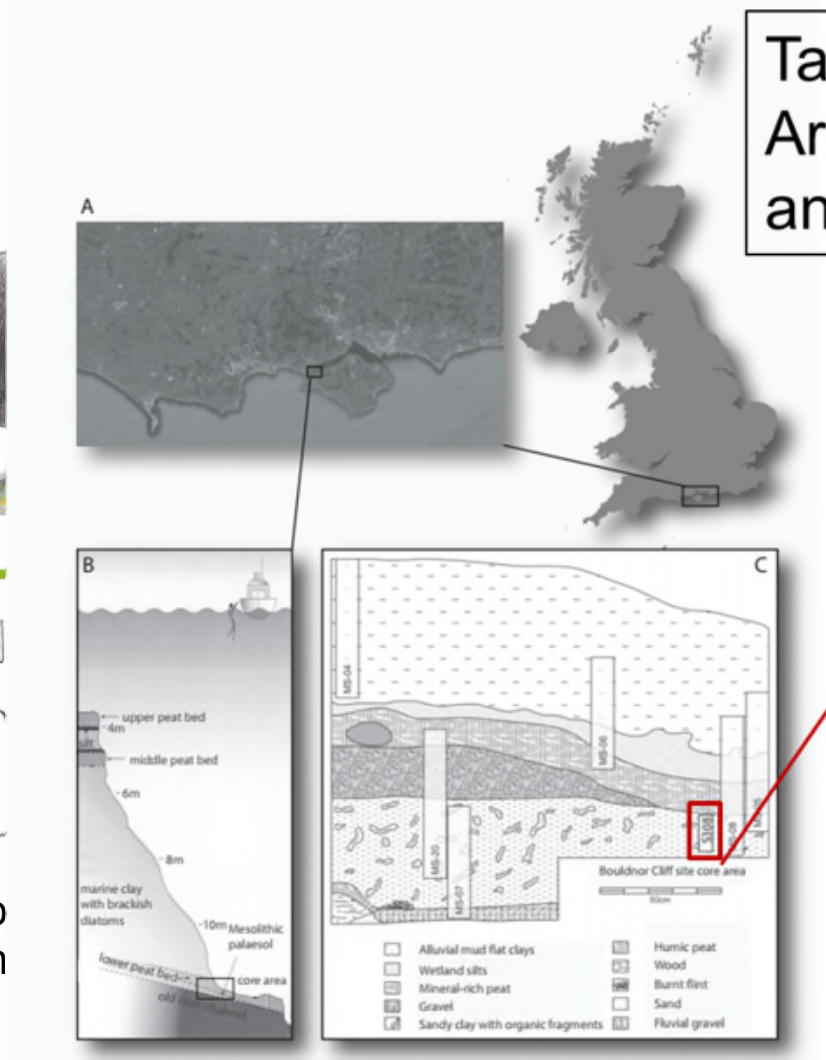

Taking a new look at Ancient flora: Archaegenomics (Sedimentary ancient DNA)

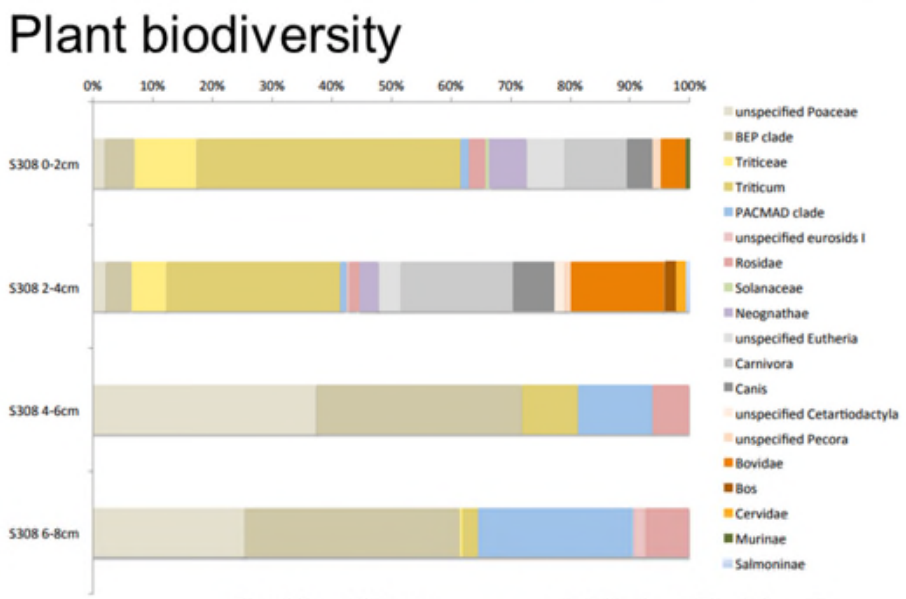

Smith, Oliver , … and Allaby, Robin G.. (2015)*Sedimentary DNA from a submerged site reveals wheat in the British Isles 8000 years ago.* Science, Volume 347 pp. 998-1001

itizen
ne for

n

Tho
Con

ing

Harnessing Diatom Community Biodiversity for Water Quality Assessment

Sampling

Water Quality Classification

DNA extraction

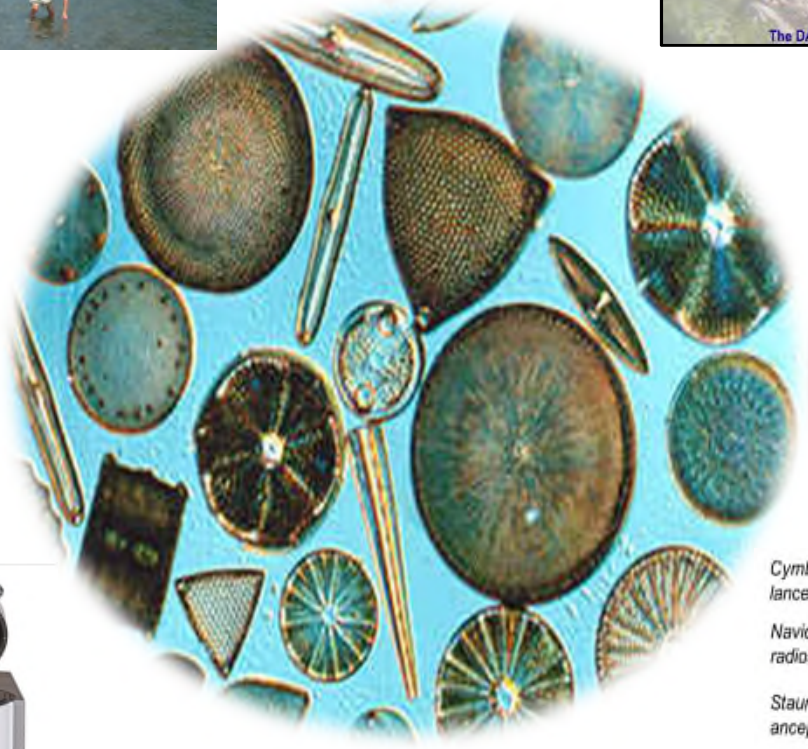

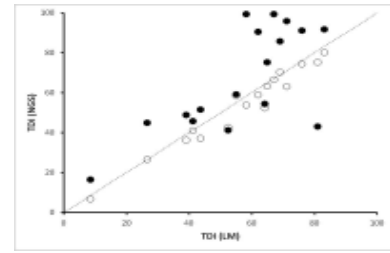

Data Interpretation

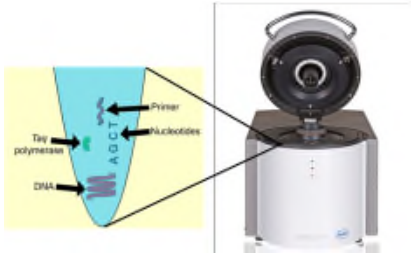

Barcode Amplification

NGS Analysis

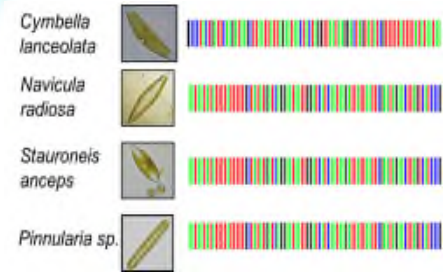

Species assignment

Metabarcoding of freshwater invertebrates to detect the effects of a pesticide spill

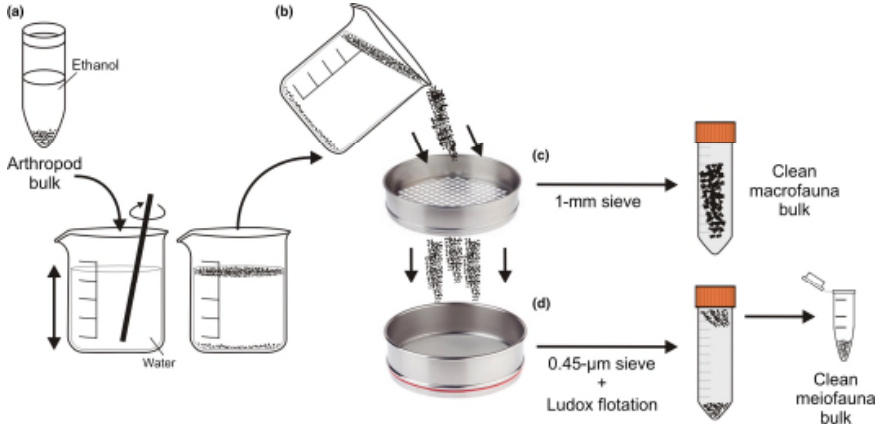

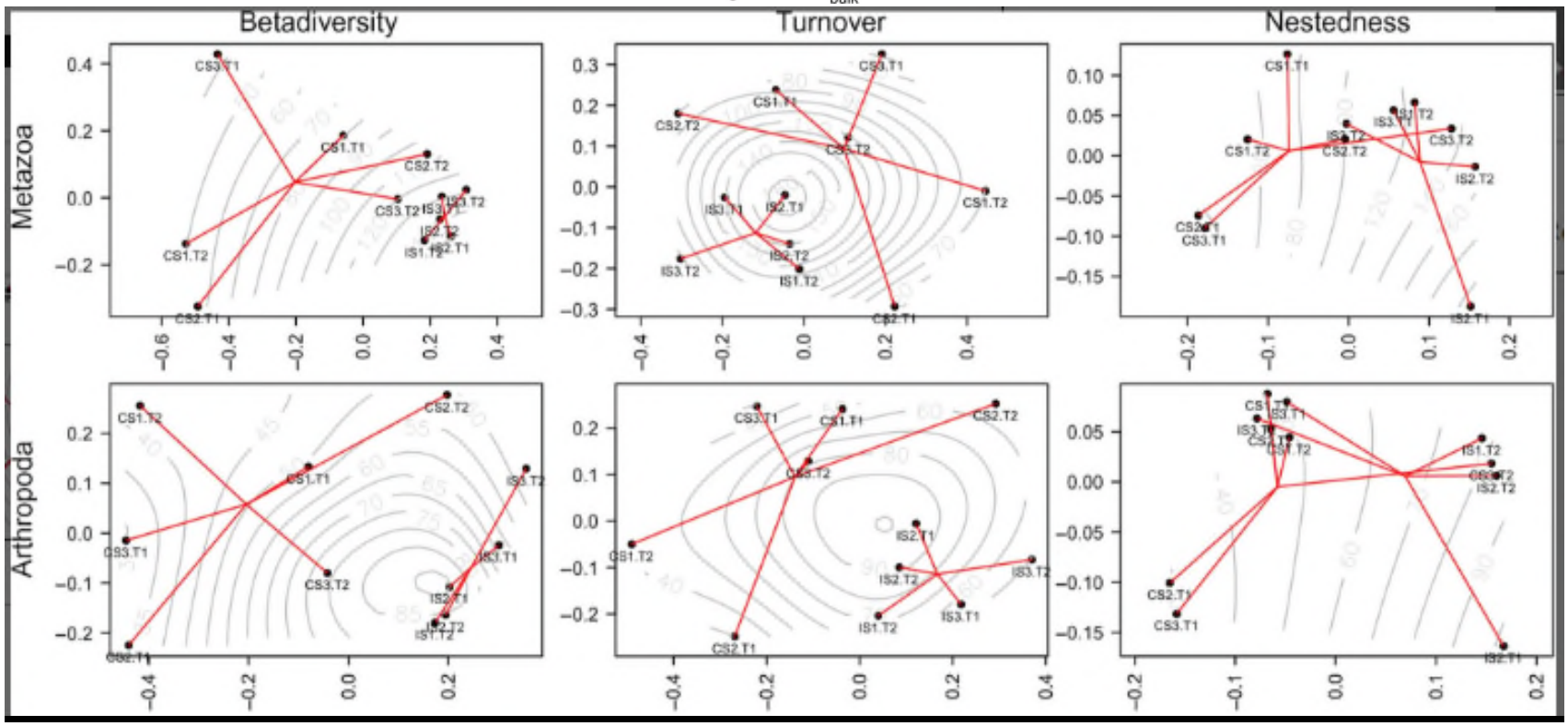

Nonparametric multidimensional scaling analyses (NMDS) based on presence/absence community matrices

Andujar et al. 2018 Molecular Ecology. 27:146– 166

A World of possibilities

Single molecule sequencing

Nanowires

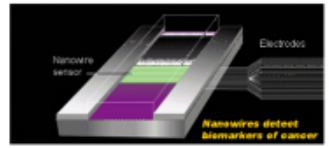

Solid State Pores

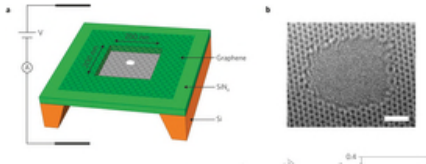

Ship-seq: Nanopore sequencing of polar microbes on board icebreakers

NERC NexUSS CDT

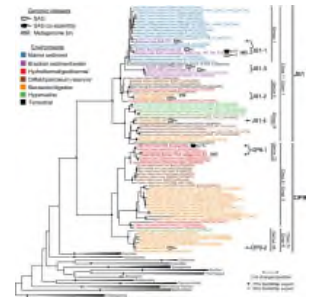

How are candidate phylum JS1 bacteria adapted for life in the deep sub-seafloor biosphere?

Weightman and Kille (2012-2015) NERC NE/J011177/1

Single cell sequencing

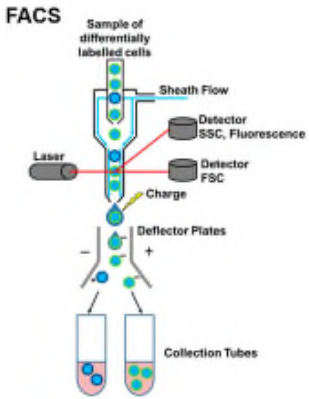

10-100 >>>>>>>>>>>1000-10,000

Summary

- Species-conservation of targets and evaluation of possible comparative toxicodynamic responses
- Species conservation of biotransformation enzymes and transporters for prediction of comparative toxicokinetic processes
- Identification key sub-lethal 'effect pathways' with clear mechanistic links to adverse outcomes
  - Issue with mapping invertebrate genes onto mammalian pathways
- Unsupervised clustering of 'omics data in a core suite of surrogate species to support chemical classification and grouping
- Retrospective monitoring of holistic ecological community impact using metagenomic profiling (eDNA)